# RADIO FREQUENCY GLOW DISCHARGE SPUTTERING OF THIN FILMS

by

Timothy John Peters

---

A Thesis Submitted to the Faculty of the

COMMITTEE ON OPTICAL SCIENCES

In Partial Fulfillment of the Requirements
For the Degree of

MASTER OF SCIENCE

In the Graduate College

THE UNIVERSITY OF ARIZONA

1 9 7 3

STATEMENT BY AUTHOR

This thesis has been submitted in partial fulfillment of requirements for an advanced degree at The University of Arizona and is deposited in the University Library to be made available to borrowers under rules of the Library.

Brief quotations from this thesis are allowable without special permission, provided that accurate acknowledgment of source is made. Requests for permission for extended quotation from or reproduction of this manuscript in whole or in part may be granted by the head of the major department or the Dean of the Graduate College when in his judgment the proposed use of the material is in the interests of scholarship. In all other instances, however, permission must be obtained from the author.

SIGNED: Timothy John Peters

APPROVAL BY THESIS DIRECTOR

This thesis has been approved on the date shown below:

Victor A. Wells

VICTOR A. WELLS
Research Associate
in Optical Sciences

Dec 3, 1973

Date

ACKNOWLEDGMENTS

The author wishes to thank the personnel of the Solid State Engineering Laboratory of The University of Arizona for their assistance and advice. In particular, he wishes to thank Dr. Victor Wells and Mr. Leonard Raymond for their advice and guidance during the preparation of this thesis.

TABLE OF CONTENTS

TABLE OF CONTENTS--Continued

LIST OF ILLUSTRATIONS

LIST OF ILLUSTRATIONS--Continued

LIST OF TABLES

ABSTRACT

This thesis contains the results of rf glow discharge sputtering of thin films. The sputtering targets used were tantalum, chromium, zinc, and zinc oxide, and these targets were sputtered in both an argon and an argon-oxygen atmosphere. In order to understand and optimize the rf sputtering system available, the parameters associated with the system were varied and the corresponding results were analyzed. The system parameters studied were the dependence of the deposition rate on the pressure of the sputtering gas, target-substrate separation, input power, deposition time, and oxygen content of the sputtering gas. The deposited films were analyzed for their uniformity in thickness, sheet resistance, and index of refraction. From the results presented in this thesis, thin films with the desired thickness, and with the electrical and optical properties investigated, can be sputtered. Some of the deposited films were evaluated for use in optical integrated circuits.

# CHAPTER 1

## INTRODUCTION

The phenomenon of sputtering has been known for over 100 years. Sputtering was first observed in the 1850's, when it was noticed that the metal of the electrodes was transferred to the glass of a discharge tube. A few years later, sputtering was proposed as a means of depositing thin films, but because the sputtering system was complicated and the films were contaminated, it was not considered a desirable method for depositing thin films. But the need arose in the 1950's to deposit nonmetallic films, and this led researchers to study the sputtering phenomenon. Today, inexpensive and well designed sputtering systems are available, and sputtering has gained acceptance as a method for depositing thin films (Blevis, 1964, pp. i-iii; Seeman, 1965, p. 1).

To give the reader a basic understanding of the sputtering process, some of the techniques of sputtering are presented in Chapter 2 of this thesis. The techniques discussed are diode sputtering, triode sputtering, rf sputtering, and reactive sputtering. If more information on these techniques is desired, the references listed at the end of each paragraph should be examined.

The purpose of this thesis is to investigate both rf nonreactive and rf reactive modes of sputtering with the system available in the Solid State Engineering Laboratory. In Chapter 3, the equipment and materials used for rf sputtering are discussed, as well as some of the

considerations that must be taken in designing a rf sputtering system. In Chapter 4, the results obtained for the nonreactive sputtering of tantalum, chromium, zinc, and zinc oxide targets are presented. Finally, in Chapter 5, the results for the reactive sputtering of these targets in oxygen are given. The parameters of the system investigated in Chapters 4 and 5 are the dependence of the deposition rate on the pressure of the sputtering gas, target-substrate separation, input power, deposition time, and oxygen content of the sputtering gas. The deposited films were evaluated for their uniformity in thickness, sheet resistance, and index of refraction.

CHAPTER 2

SPUTTERING THEORY

Sputtering occurs when momentum is transferred between the ions in a gas discharge and the atoms of the target. The sputtered atoms are then deposited as a thin film on the surrounding surfaces. The means by which the gas discharge is formed determines the sputtering method being used. A diagram of the basic sputtering methods is shown in Fig. 1.

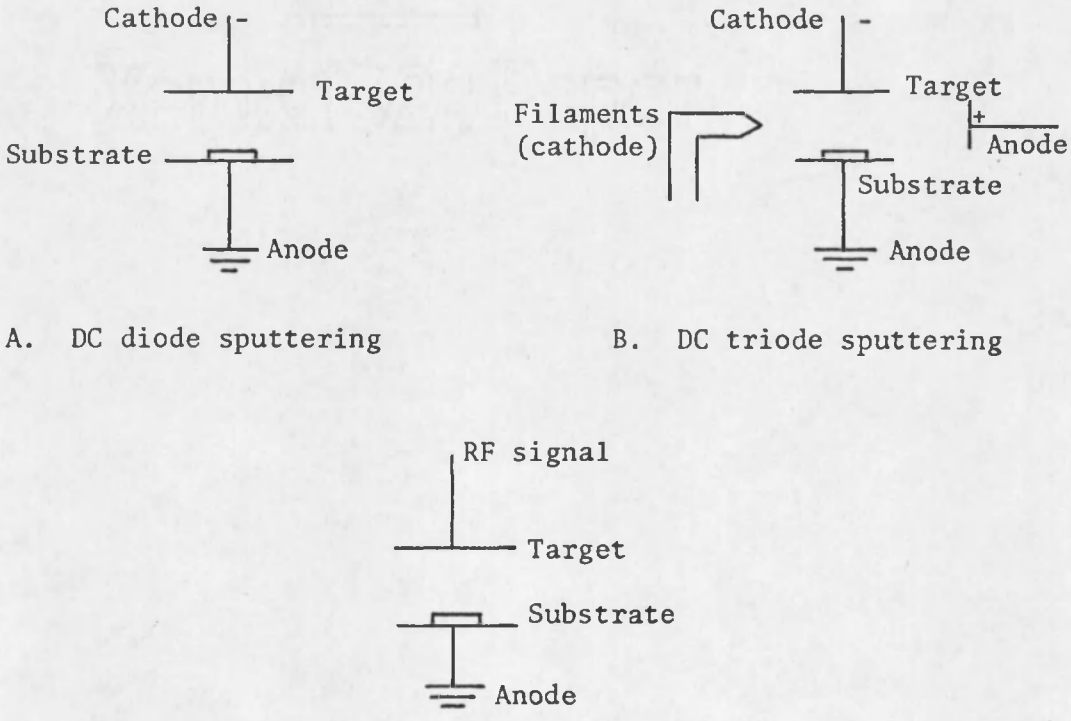


A. DC diode sputtering

B. DC triode sputtering

C. RF diode sputtering

Fig. 1. Modes of Sputtering.

From Froemel and Sapoff, 1967, p. 34.

In dc glow discharge, or diode, sputtering, a high negative potential, around 1000 to 3000 V, is applied to the target. This negative potential repulses electrons from the target, which collide with the gas molecules in the sputtering chamber, forming the gas discharge, or plasma. Once the plasma is created, this negative potential also forms an electron-free region, or ion sheath, around the target. Ions from the plasma are attracted to the target, owing to its negative potential, pass through the ion sheath, and are accelerated to the target. This ion bombardment of the target results in the target atoms being sputtered. (See Blevis, 1964.)

To avoid collisions between the sputtered and accelerated atoms, and to avoid gas entrapment in the deposited film, the discharge should take place in a low-pressure atmosphere. For this reason, triode sputtering is advantageous to diode sputtering. In diode sputtering, in order to maintain a discharge, the ions must free secondary electrons from the target. These electrons further ionize the gas in an avalanche type process, which requires high pressures. This is not needed for triode sputtering because the electrons are continuously being supplied by the thermionic emitter (Blevis, 1965, pp. 10-11).

In triode sputtering, the target is a third element in the system, independent of the plasma formation. The plasma is formed by the electrons emitted from the thermionic emitter, which is usually a filament, and are accelerated to an anode. As they are accelerated, the electrons ionize the gas, and sputtering takes place as described previously. Filaments are used because they have a low negative potential, which means that very little sputtering will occur from them. Because

in triode sputtering the filaments are continuously supplying electrons, the gas in the sputtering chamber can be ionized at a pressure that is 100 times less than in diode sputtering (Nickerson and Moseson, 1965).

When the target is an insulator, direct current (dc) sputtering will not work because no net dc current can flow through it. This means that no dc current can be drawn to the target, and dc sputtering cannot take place because there is no accelerating potential. But, if a radio frequency (rf) potential is applied to the target, a displacement current may flow through the target, and sputtering can occur.

In rf sputtering, positive ions in the plasma reach the target during the negative portion of the rf cycle, and electrons reach the target during the positive portion of the rf cycle. Owing to its mass and charge, the mobility of the electrons is about $10^5$ greater than that of the positive ions, and more electrons than ions will reach the target (see Fig. 2). This means that the target's surface will be negatively charged. After several rf cycles, an equilibrium situation occurs where the target is at a negative dc bias, and equal electron and ion currents are drawn to it in one rf cycle. This negative potential on the target's surface repels the electrons from the target, creating an ion sheath similar to that encountered in dc sputtering, and again sputtering occurs. If a metal target is to be rf sputtered, a blocking capacitor must be placed in the input line in order to prevent a net flow of direct current, thus allowing a negative bias to build up on the target. If the frequency of the applied voltage is too low, enough ions will reach the target during the negative half of the rf cycle to neutralize the negative charge on the target. If this occurs, no negative dc

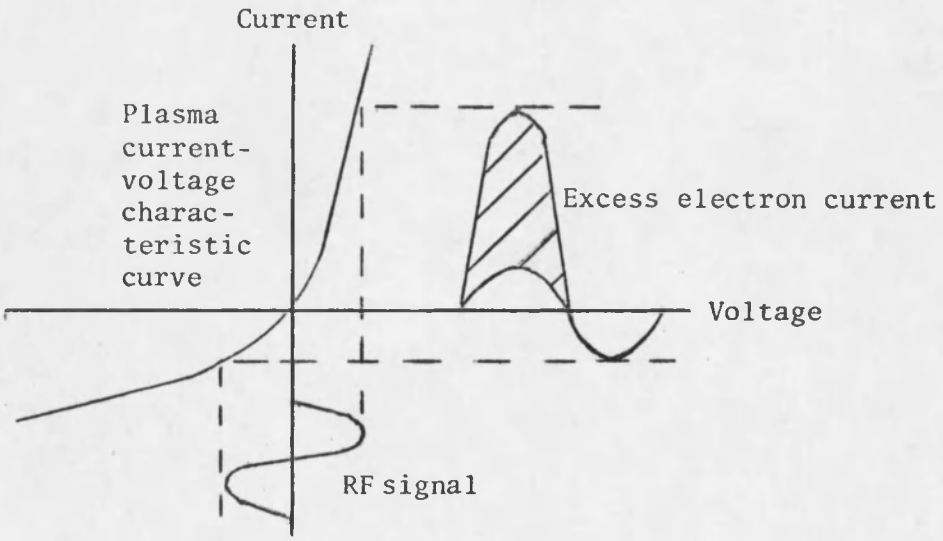


A. When RF Signal Is First Applied.

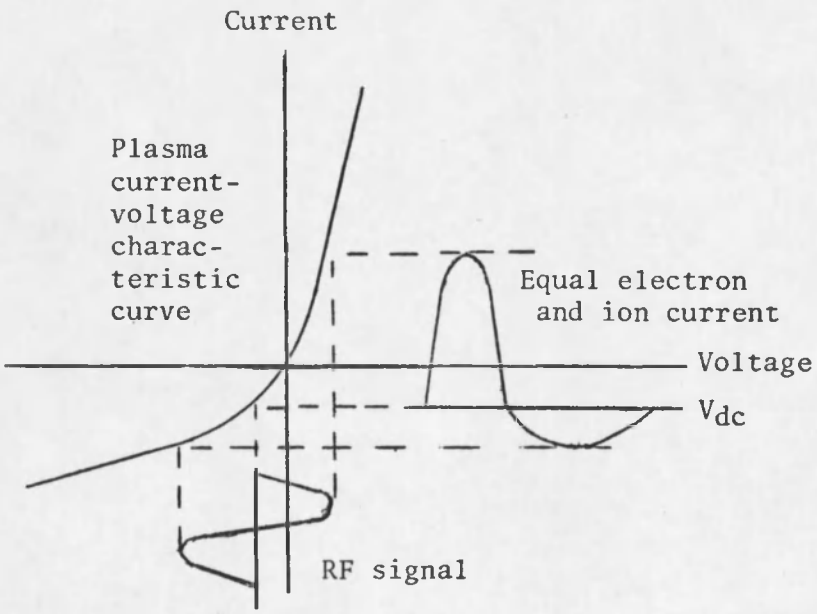


B. After Equilibrium Is Reached.

Fig. 2. Diagram of Sheath Formation for RF Sputtering. After Vossen and O'Neill (1968, p. 153).

potential will build up, and the target will not be sputtered. The lowest frequency that can be used to create an ion sheath is 10 kHz. At higher frequencies, fewer ions reach the target in one cycle, and this increases the negative bias. But owing to the effective capacitance and inductance of the plasma and input leads, and owing to the problem of grounding, the highest frequency that should be used to maintain a stable plasma is 10 to 20 MHz. The only frequency in this range allowed by the FCC for scientific use is 13.5 MHz; thus, this is the frequency most commonly used for rf sputtering (Vossen and O'Neill, 1968; Cash, Cunningham, and Keene, 1967; Davidse, 1966; Blevis, 1965).

An advantage of rf sputtering is its versatility because both insulators and metal targets can be sputtered with the same equipment. The disadvantages of rf sputtering are that extra care must be taken in adequately grounding the system. Also, short, large-area input wires are needed in order to avoid excessive input impedance. The sputtering chamber must be symmetric and not have sharp corners, to avoid high electric field concentrations. Finally, care must be taken in matching the impedance of the leads and discharge to that of the rf generator (Vossen and O'Neill, 1968).

There are two means by which films containing more than one element can be sputtered. One way is to sputter the compound target in an inert gas, and the other way is to reactive sputter a target composed of one of the elements. Reactive sputtering can be done provided that the other elements can be easily obtained in the gaseous state. In reactive sputtering, an inert sputtering gas, i.e., a gas that will not react with the sputtered atoms, is mixed with a reactive gas. A common inert

gas is argon, and two common reactive gases are oxygen and nitrogen. Reactive sputtering occurs because reactive gases are characteristically electronegative and the atoms sputtered from the target are in a highly energetic state; thus, they are very likely to react with the negative atoms. The deposited film is a mixture of the sputtered atoms and reactive gas. By varying the amount of reactive gas in the sputtering chamber, the resultant film will contain a different amount of the sputtered atoms-reactive gas mixture, and will exhibit different properties (Vossen and O'Neill, 1968, p. 151).

The main advantage of reactive sputtering is that a single target can be used to produce several different types of films. Several different compound targets, which are sometimes difficult to obtain in bulk form, are not needed when different mixtures of the given elements need to be examined. Also, reactive sputtering has the effect of diluting the contribution of undesired gases that may be present when a target is sputtered (Vranty and Harington, 1965, p. 486).

The disadvantage of reactive sputtering is the low deposition rates. This occurs for two reasons. The atomic mass of the reactive gas is usually small, with the result that the momentum transfer between the ions and the target material is less than when argon is used as the sputtering gas. Also, reactive gases are characteristically electronegative; they tend to capture the secondary electrons, which, as discussed previously, are also emitted by the ion bombardment. These two factors result in a lowering of the deposition rate (Schwartz, 1966, p. 87).

In this thesis, rf nonreactive sputtering and rf reactive sputtering of tantalum, chromium, zinc, and zinc oxide are studied.

CHAPTER 3

EQUIPMENT AND MATERIALS

The equipment and the materials used to investigate rf sputtering of thin films are discussed in this chapter. Also, some of the design considerations of sputtering systems are discussed.

A block diagram of a rf sputtering system is shown in Fig. 3.

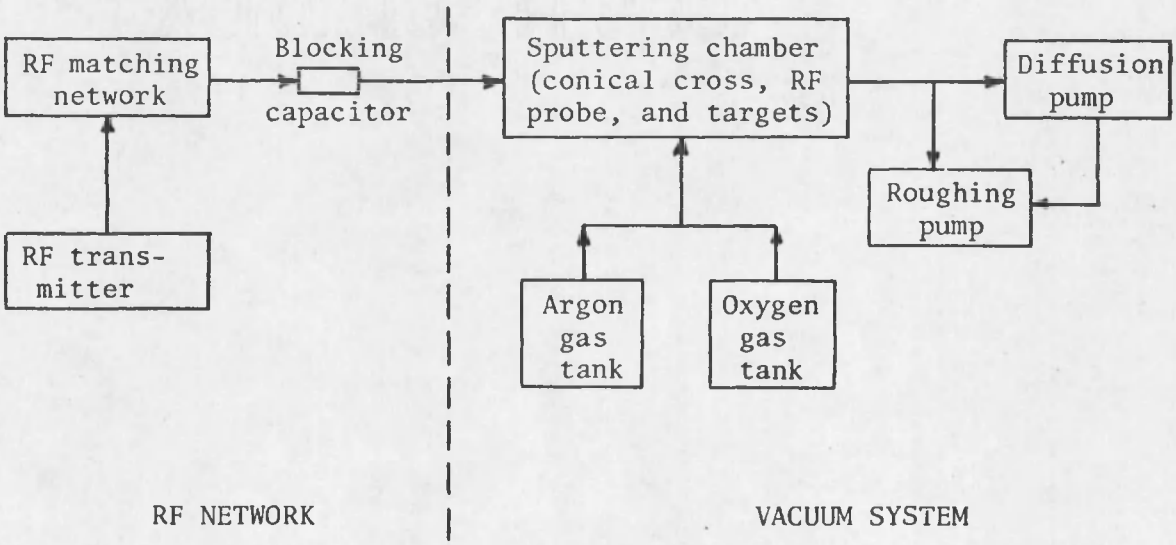


Fig. 3. Block Diagram of RF Sputtering System.

The system can be divided into two main sections, the rf network and the vacuum system. The rf network consists of a 13.5 MHz rf transmitter and a matching network. The rf transmitter provides the power needed for

sputtering, and the matching network matches the output impedance of the transmitter with the load so that the maximum amount of power is supplied to the targets. The vacuum system consists of a roughing pump and a diffusion pump, which are used to evacuate the sputtering chamber. Inside the sputtering chamber, which for this system is a conical cross, the target is mounted on a copper probe, which conducts the power supplied from the transmitter. The sputtering gas is fed into the sputtering chamber by means of a micrometer valve.

## The RF Network

The rf transmitter was a modified Collins rf transmitter, which was tuned for 13.5 MHz for the experiments done for this thesis. The maximum output power used to deposit the films in this investigation is 250 W. The power was limited by the excessive heating of the target, conical cross, and the electrical components in the network.

The matching network consisted of a variable capacitor and an inductor, which were used to tune the matching network so the maximum power went into sputtering the target. All connecting wires were either rf wire or rf ground straps. Special wiring is needed because the rf power tends to travel along the surface of the conducting wire, which means that the wire needs to have a large surface area. To avoid excessive impedance, the wiring needs to be short.

The need for the blocking capacitor has already been discussed in Chapter 2. Without this capacitor, metal targets could not be sputtered.

Good grounding is a necessity for rf sputtering at 13.5 MHz. Otherwise the standing wave ratio (SWR) is high, and everything associated with the system is electrically activated by the rf power. In order to achieve good grounding, rf grounding straps were connected directly from the bottom of the substrate platform to the external ground through the base plate; this is shown in Fig. 4. The aluminum supports did not provide an adequate conduction for the 13.5 MHz rf frequency. To avoid dissimilar connections, all of the connections through the system to ground were copper. With adequate grounding, the SWR was brought down to an acceptable level.

## The Vacuum System

The sputtering chamber consisted of a Pyrex conical cross (Fig. 4). The vertical arm is 6 in. in diameter and 18 in. high; the horizontal arm is 4 in. in diameter and 16 in. long. A conical cross was used to reduce the volume required to be evacuated and to provide convenient handling of the vacuum chamber.

The conical cross was evacuated using a high-vacuum roughing pump and a 6-in. diffusion pump (see Appendix A on the procedures of operating the sputtering system). The pressure in the conical cross was read by means of a thermocouple located in the base plate, and the pressure in the diffusion pump was read by means of an ionization gauge located at the top of the diffusion pump.

The temperature of the substrate and platform was taken during the trials by means of two copper-constantan thermocouples, and read through the use of a potentiometer.

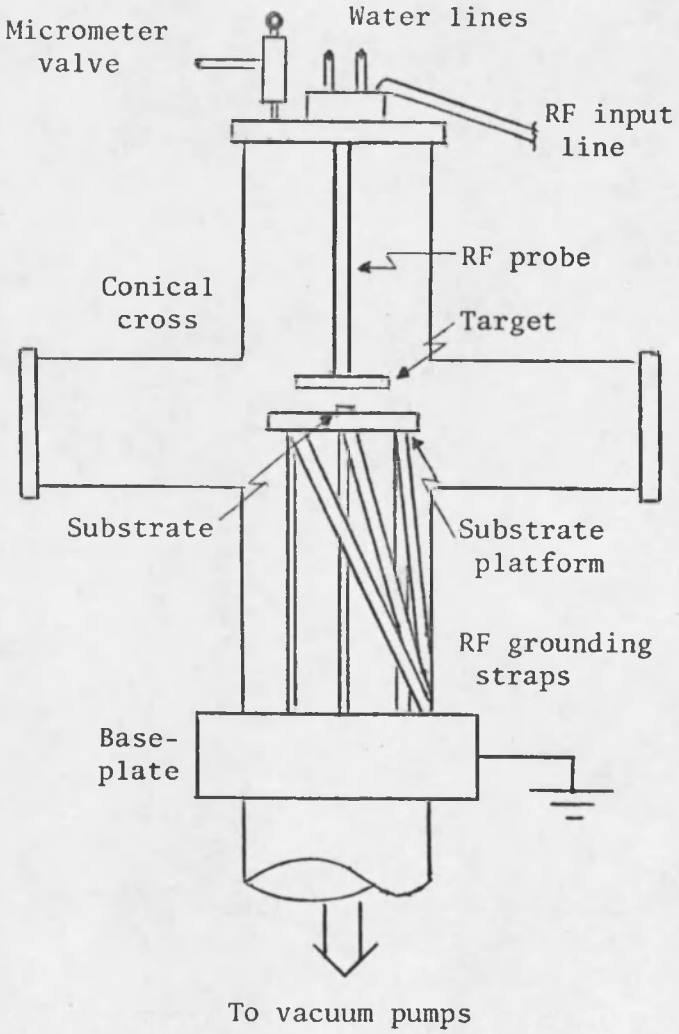


Fig. 4. Conical Cross.

The gas feed lines were all copper tubing except for the line used to make the final connection to the micrometer valve on top of the conical cross. This line had to be made of tygon tubing in order to prevent the rf power from traveling to the gas tanks.

All of the targets were 5 in. in diameter except for the chromium target, which was 5½ in. in diameter. There are several important considerations that must be taken into account in designing a target for rf sputtering. Faster rate and more even depositions result from larger targets because there is more surface area from which sputtering takes place, and because the sputtered atoms emitted at small angles are more evenly collected. The targets should be round to avoid excessive rf power losses that occur from the corners of a square target. The target should not be any thicker than ¼ in. to avoid the problems of cooling the front surface of the target and to limit the loss of the rf power through the target. Higher deposition rates are achieved with rougher targets because of the increased surface area. Finally, epoxy binding of a target, as was done for the zinc oxide target, should be avoided whenever possible. Water cooling of the target is essential to avoid loss of epoxy strength and outgassing of the epoxy. In addition, the epoxy must be evenly distributed because a small unbounded region can cause hot spots that can lead to failure of the epoxy bond or fracture of the target. The backing material must have a high electrical and thermal conductivity and a very low sputtering deposition rate (Murray and Class, 1970).

The target was attached to a copper probe, by which the rf power was conducted from the input wiring to the target. A glass shield fits

around the probe so that no sputtering will occur from the copper probe itself.

All of the films studied were deposited on glass and/or silicon substrates. The glass substrates were microscope slides. The advantages of glass substrates are that they are easy to obtain and have a smooth surface; the disadvantages are that they have poor thermal conductivity and are easily broken (Murray and Class, 1970, p. 115).

Thus, the essential design of the system used in these investigations, and some of the considerations that must be taken into account in designing a sputtering system, have been described. In Fig. 5A, a photograph of the sputtering chamber used for the experiments in this thesis is shown. Figure 5B is a photograph of this chamber when the plasma is formed in it.

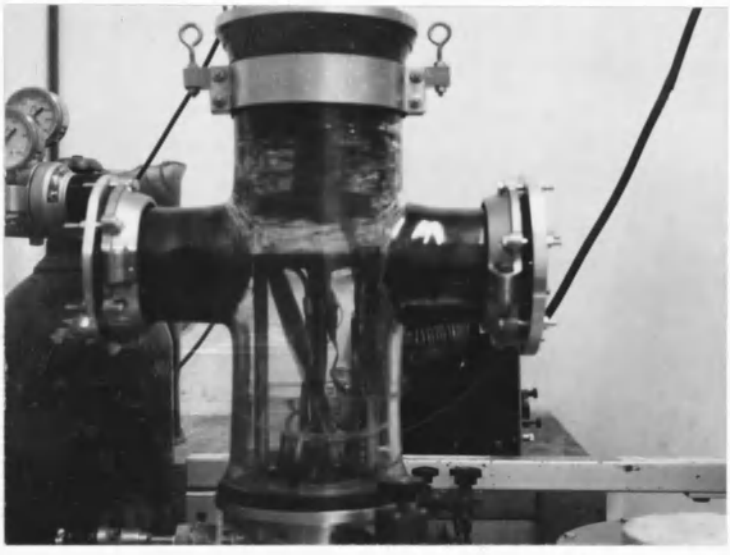

A. Before Plasma Formation.

B. After Plasma Formation.

Fig. 5. Sputtering Chamber.

# CHAPTER 4

## NONREACTIVE RF SPUTTERING OF TANTALUM, CHROMIUM, ZINC, AND ZINC OXIDE

In this chapter, the results obtained for the sputtering of tantalum, chromium, zinc, and zinc oxide targets in an argon atmosphere are discussed. In the next chapter, the results obtained for the reactive sputtering of these targets in an argon-oxygen atmosphere are discussed. To obtain these results, one parameter was varied while all of the other parameters associated with the system were held constant. Of concern was how the deposition rate depended on the pressure of the argon gas, the target-substrate separation, the applied power, and the deposition time. Also of interest for the zinc oxide target was the variation of the deposition rate when the substrate was not cooled.

The deposited films were measured for their sheet resistance and thickness. The sheet resistance of the films was measured with a four point probe. The thickness of the films was measured through the use of Fizeau fringes, which are fringes of constant thickness. A step was created in the film, and the displacement of these fringes was observed with a microscope. (See Appendix B on the procedure used to measure the thickness of the film.)

The results of the rf sputtering of tantalum, chromium, and zinc are expected to be similar because they are metal targets. The results

for the zinc oxide target are expected to be different because it is an insulating target.

## Deposition Rate vs Pressure

The first parameter to be examined is the variation in the deposition rate with the pressure of the gas in the sputtering chamber. From Figs. 6 and 7 it can be seen that the deposition rate is dependent on the pressure. The values of the pressure stated are the corrected values from the meter readings. This correction is needed because the meter indicates pressure based on air, and argon is used in the nonreactive sputtering of these targets.

From these graphs, it can be seen that the pressure where the maximum deposition rate occurred varied with the target material. This variation is dependent on the atomic mass of the sputtered atom. The maximum deposition rate of tantalum, which has an atomic mass of 181, occurred at a pressure near 9 μm. For chromium, which has an atomic mass of 52, and zinc, which has an atomic mass of 65, the maximum deposition rate occurred at a lower pressure, near 5 μm. These results are expected when it is remembered that the principal mechanism for sputtering is momentum transfer. Chromium and zinc sputtered at a lower pressure than tantalum because, when the target atoms have a smaller atomic mass, it takes fewer ions to release them. Therefore, sputtering occurs at a lower pressure.

From these graphs, it is seen that the deposition rate is dependent on the target-substrate separation. This would be expected because the potential drop between the electrodes decreases when the

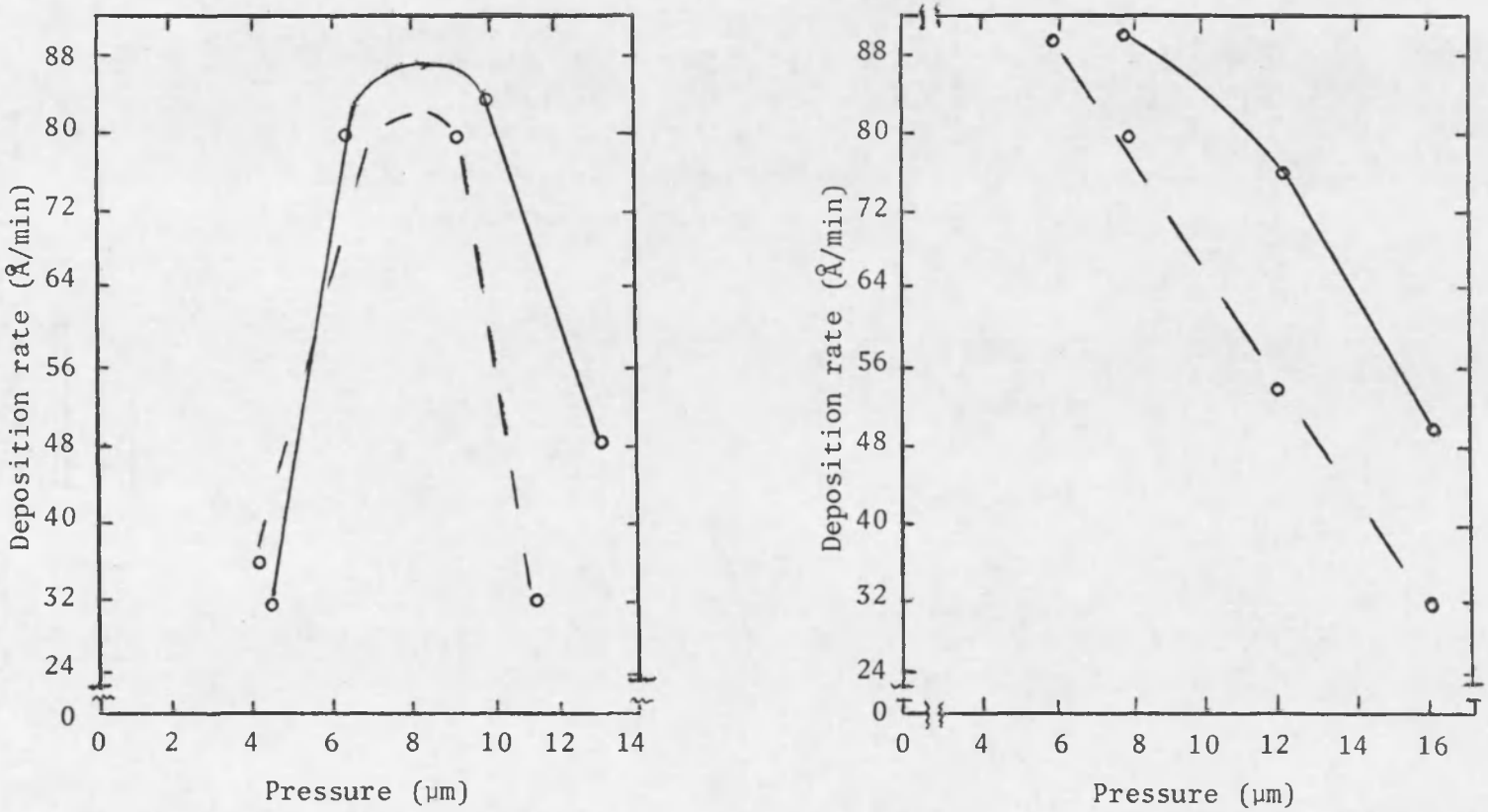


Fig. 6. Deposition Rate vs Pressure for Tantalum and Chromium.

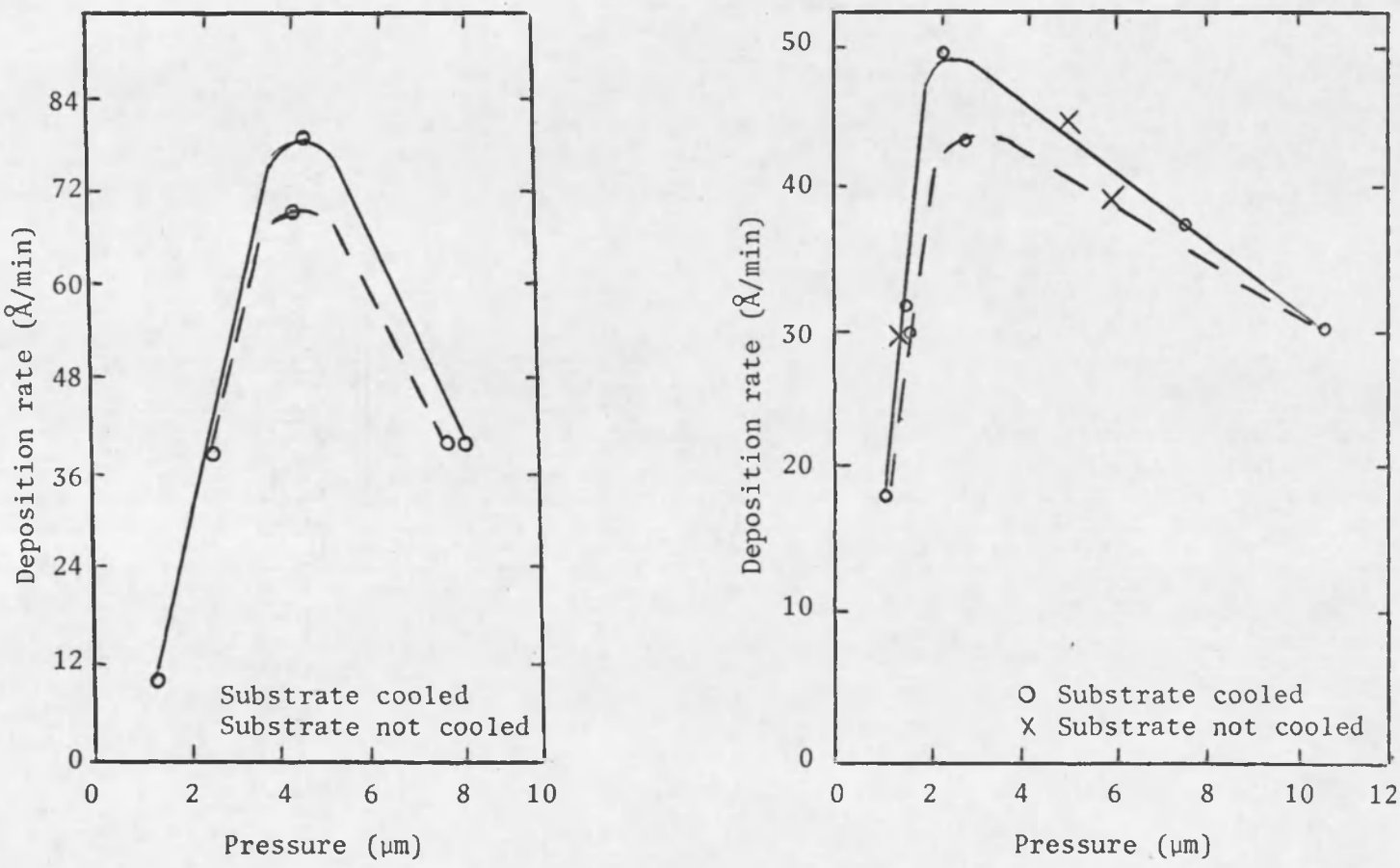


__ 1½-in. target-substrate separation
-- 2-in. target-substrate separation

A. Zinc

__ 1½-in. target-substrate separation
-- 2-in. target-substrate separation

B. Zinc Oxide

Fig. 7. Deposition Rate vs Pressure for Zinc and Zinc Oxide.

separation between them increases. Therefore, the ions bombard the target with less energy, which leads to a lowering of the deposition rate.

It is also observed from Fig. 7 that the zinc oxide target sputters at a lower deposition rate, and at a lower pressure, than the metal targets. This occurs because some of the power is lost due to the insulating nature of the target. Thus, although 250 W is applied to the target, the potential drop between the electrodes in the sputtering chamber is less than when the target is a conducting material. With a decrease in the potential drop, the mean free path of the sputtered atoms is less because less momentum is transferred to them by the ions. This means that sputtering must occur at a lower pressure and that there is a subsequent decrease in the deposition rate.

From the results with zinc oxide, it is seen that the deposition rate is independent of whether or not the substrate is cooled. This is expected because the potential drop between the electrodes should be independent of whether the substrate is or is not cooled. Therefore, the deposition rate should not be affected. However, as is discussed in Chapter 5, the index of refraction did change.

## Deposition Rate vs Input Power

The next parameter to be examined is the dependence of the deposition rate with the rf power applied to the target. The input power was taken as the difference between the forward and the reflected power. Figure 8 shows graphs of the deposition rate as a function of the input power per square centimeter of target surface. This normalization is used because the sputtering rates vary with the surface area of the

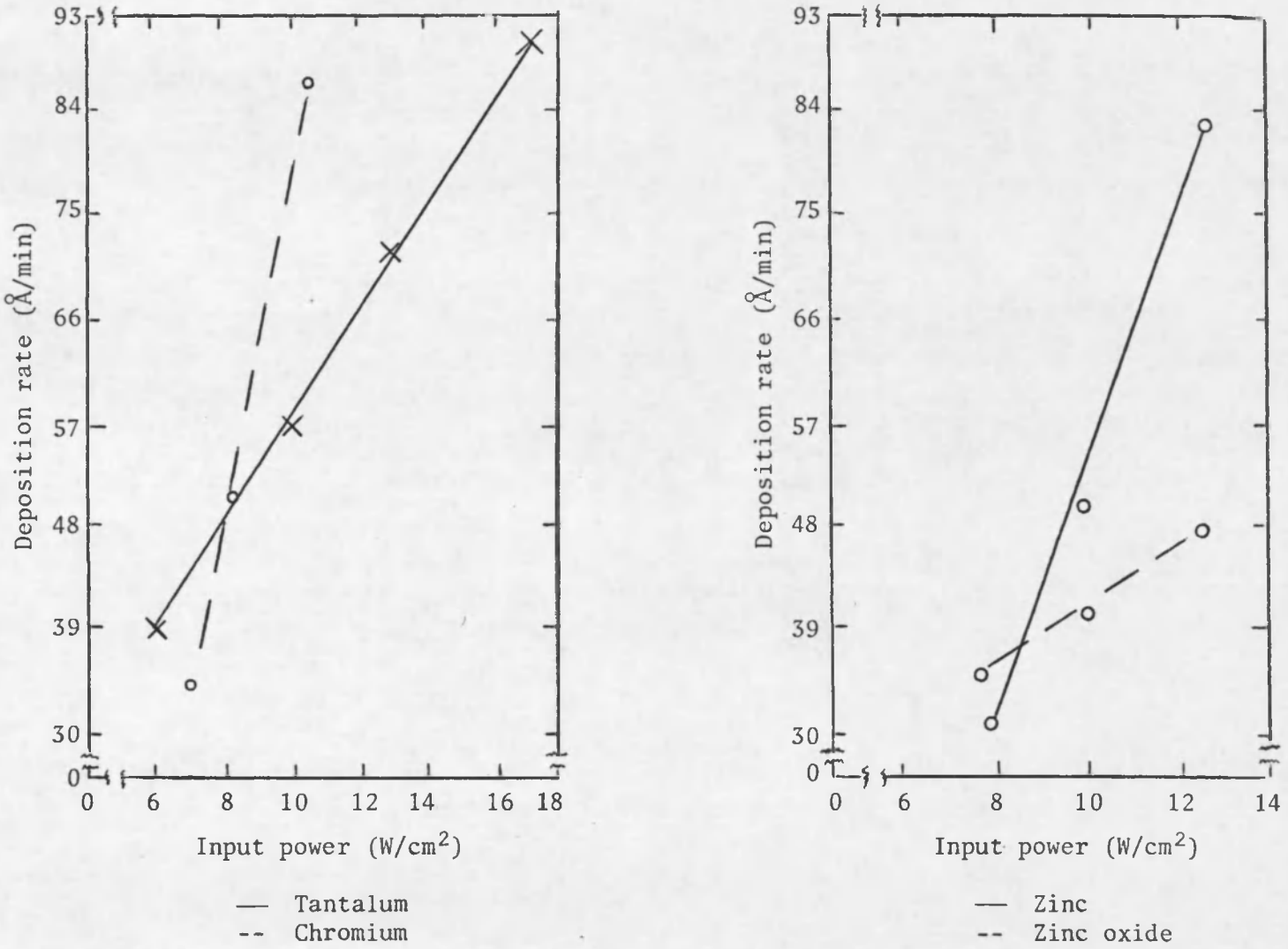


Fig. 8. Deposition Rate vs Input Power for Tantalum, Chromium, Zinc, and Zinc Oxide.

target. But the chromium target is 5½ in. in diameter, compared to the 5-in. diameter of the other targets. This difference in the target surface area is normalized out by plotting the deposition rate as a function of the input power per square centimeter of target surface.

For the chromium target, an input power of 250 W corresponds to 10.4 W/cm$^2$ on the horizontal scale of the graphs in Fig. 8. For the tantalum, zinc, and zinc oxide targets, 250 W corresponds to 12.7 W/cm$^2$ on these graphs.

It is seen from the curves in Fig. 8 that the deposition rate increased linearly with increasing input power. However, the rate of change of this increase varied with the target material, the change being greater for tantalum than for chromium.

This variation is expected when the atomic mass of the target atoms is considered. For higher input power, more secondary electrons are emitted from the chromium target than from the tantalum target because it takes less transfer of momentum from the argon ions to release the chromium atoms, which have lighter atomic mass; therefore, more momentum is transferred to the secondary electrons. This leads to further ionization of the argon gas and results in an increase in the deposition rate. Because the tantalum atoms are more massive than the chromium atoms, the rate of change of the deposition rate with increasing input power is expected to be less. Similarly, because of the insulating nature of the zinc oxide target, it is expected to have a lower rate of change in the deposition rate with increasing input power than zinc.

The standard rf input power setting was chosen as 250 W for the remaining trials because of the heating effects of the rf power.

Excessive heating occurred at the arms of the conical cross, on the target, and on the blocking capacitor used in the matching network when the power level exceeded this value.

## Thickness vs Time

From Fig. 9 it is seen how the deposition rate varied with the time of the experimental trial. The deposition rate is the slope of the curves plotted in this figure. The curves show that the deposition rate is constant with respect to time. Consistent with the previous results, it is seen that the deposition rate is slightly lower for the rf sputtering of the tantalum target than for the chromium target. The zinc oxide target has the lowest deposition rate because of the insulating nature of the target.

## Sheet Resistance

The sheet resistance of the deposited films was measured with a four-point probe. From Fig. 10 it is seen how the sheet resistance varied with the thickness of the deposited films. The horizontal scale of these graphs is a logarithmic scale.

An inverse relationship between the sheet resistance and the thickness of the films is noted from these graphs. This is to be expected because the sheet resistance, $R_s$, of one square of film surface is

$$R_s = \rho/t \qquad (1)$$

where

$\rho$ is the sheet resistivity of the element, and

$t$ is the thickness of the deposited film.

It is measured in ohms per square (Maissel and Glang, 1970, pp. 13-15).

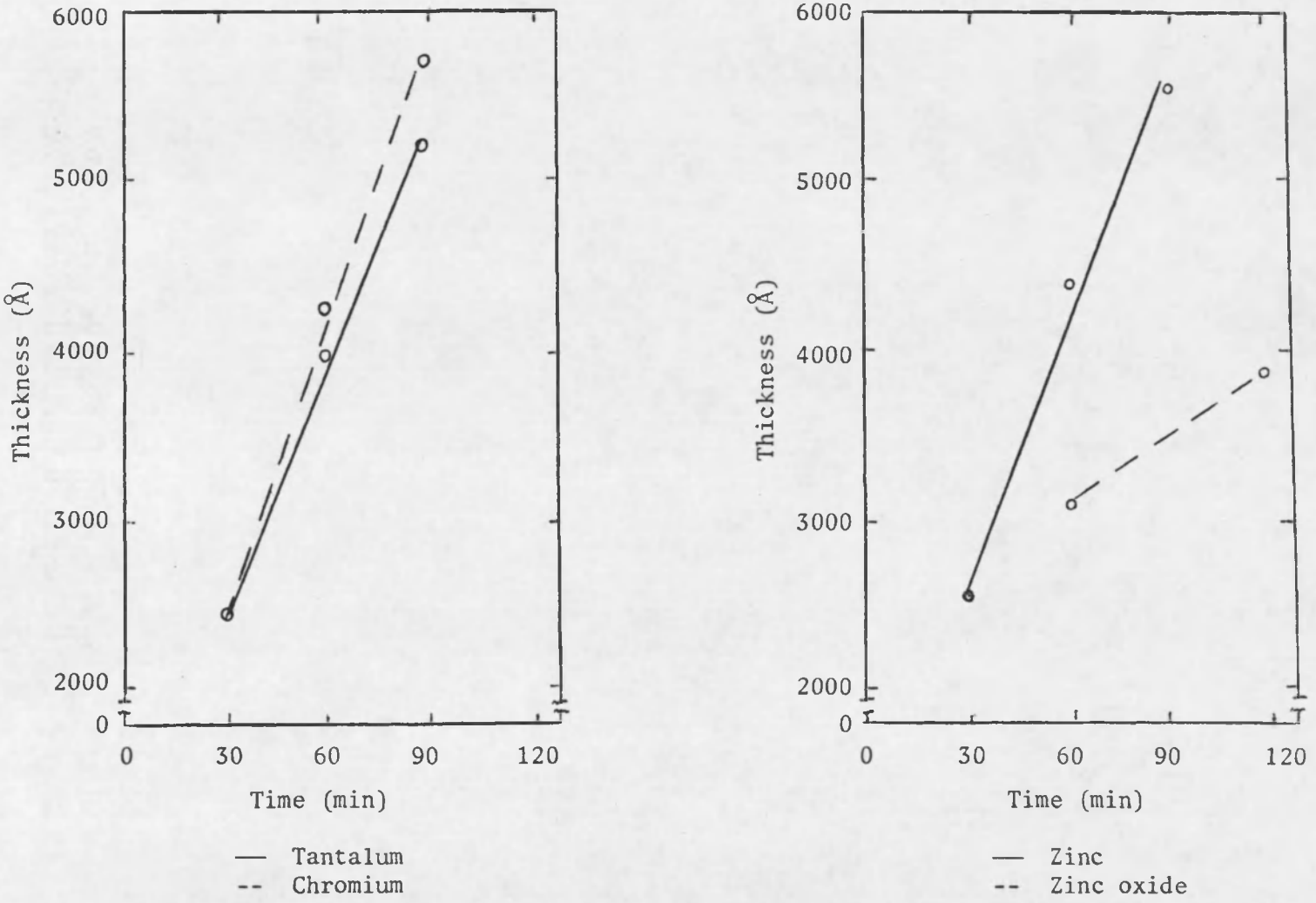


Fig. 9. Thickness vs Time for Tantalum, Chromium, Zinc, and Zinc Oxide.

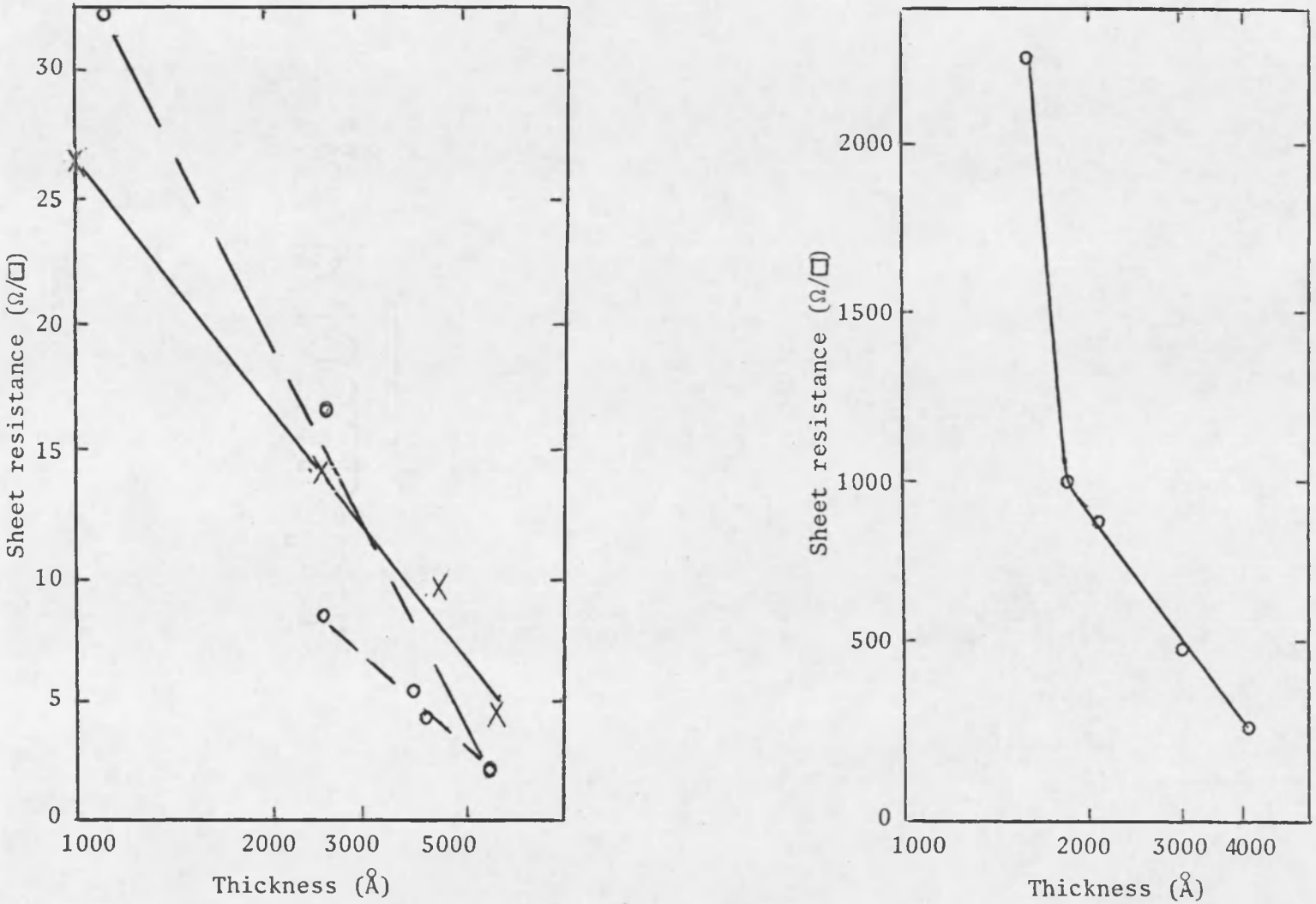


— Tantalum -- Chromium — - Zinc — Zinc oxide

Fig. 10. Sheet Resistance vs Thickness for Tantalum, Chromium, Zinc, and Zinc Oxide.

Sheet resistance is used as a measurement of the resistance of the deposited films because, as seen from Eq. (1), it is independent of the size of the square. This means that it can be compared to values of the sheet resistance made with other instruments, independent of the specifications of the instruments.

In Table 1, it is seen how the measured values of the sheet resistance differed with the theoretical values. The value of the sheet resistivity stated in Table 1 for each element is the bulk value. The measured values for the sheet resistance are much higher than the theoretical values. This is caused by several factors. There is a certain amount of argon gas incorporated into the sputtered film. Also, with thin films, there is a lack of sufficient charge carriers to carry the current. These factors will cause the sheet resistance to be higher than the theoretical values.

Because of the properties of dielectric films, they should exhibit very high sheet resistance, and this is seen in Fig. 10. The zinc oxide film had a sheet resistance that was about 200 times greater than that of the sputtered zinc film.

## Summary of the Nonreactive Sputtering of Tantalum, Chromium, Zinc, and Zinc Oxide

From these results, some of the characteristics of rf nonreactive sputtering can be seen. The deposition rate is dependent on the target material, the pressure in the sputtering chamber, the power applied to the target, and the target-substrate separation. The deposition rate remains constant as the time of deposition is increased, and

Table 1. Measured Sheet Resistance Compared to Theoretical Sheet Resistance for Tantalum, Chromium, and Zinc.

| Thickness, angstroms | $R_S$, Ω/□ | |
|---|---|---|
| | Theoretical | Measured |
| Tantalum (ρ = 12.4 μΩ-cm) | | |
| 1000 | 1.2 | 26 |
| 2000 | 0.6 | 16 |
| 3000 | 0.4 | 11 |
| 4000 | 0.3 | 9 |
| 5000 | 0.2 | 6 |
| Chromium (ρ = 12.9 μΩ-cm) | | |
| 3000 | 0.4 | 7 |
| 4000 | 0.3 | 4 |
| 5000 | 0.2 | 3 |
| Zinc (ρ = 5.9 μΩ-cm) | | |
| 2000 | 0.3 | 19 |
| 3000 | 0.2 | 11 |
| 4000 | 0.1 | 8 |
| 5000 | 0.1 | 3 |

the rate is less for an insulating target than for a metal target. The measured sheet resistance is higher than predicted theoretically, which is expected because of the nature of thin films.

In the next chapter, the reactive sputtering of the targets is examined. Also, additional properties of the nonreactive sputtering of the zinc oxide target are examined. These are properties associated with the parameters that were varied and measured for the oxides.

# CHAPTER 5

## REACTIVE RF SPUTTERING OF TANTALUM, CHROMIUM, ZINC, AND ZINC OXIDE

In this chapter, the results of sputtering the tantalum, chromium, zinc, and zinc oxide targets in an argon-oxygen atmosphere are discussed. As was done in the previous chapter, these results were obtained by varying one parameter while holding all of the other system parameters constant. The parameters examined for their effects on the deposition rate were the addition of oxygen in the sputtering gas, pressure of the sputtering gas, cooled vs uncooled substrate, target-substrate separation, applied power, and deposition time. The variation in deposition rate with position on the substrate platform was also examined.

The deposited films were measured for their thickness, sheet resistance, and index of refraction. The thickness of the films was measured by use of Fizeau fringes and a step in the film. The sheet resistance of the films was measured with a four-point probe. The refractive index of the films was measured by the use of spectrophotometric transmission curves. (See Appendix C on how the index of refraction was determined.)

### Deposition Rate vs Oxygen Content

The first parameter to be examined is the variation in the deposition rate with the oxygen content of the sputtering gas. As the particular gas was added, the argon-oxygen mixture was determined by reading

the pressure in the sputtering chamber. No attempt was made to correct the meter reading, so all of the values are stated as they were read from the meter.

As explained in the theory of reactive sputtering, it is expected that the deposition rate will decrease with increasing oxygen content in the sputtering gas. The curves in Fig. 11 show that this occurred. It should be noted that the graphs also reveal a leveling of the deposition rate with increasing oxygen content in the sputtering gas. This indicates that an equilibrium condition exists between the number of secondary electrons emitted by the ion bombardment of the target and those captured by the reactive gas. Two of these levels are noted for the reactive sputtering of the tantalum target. This is probably due to the small number of secondary electrons emitted from this target.

As discussed previously, more secondary electrons are emitted when the chromium target is sputtered. From these curves, it is seen that, as oxygen is added to the sputtering gas, the deposition rate decreases much more rapidly for the chromium target than for the tantalum target. This indicates that, as soon as the atomic mass of the sputtering gas decreases, fewer secondary electrons are emitted from the target, which is expected because the momentum transfer is less. However, as seen in Fig. 11, when the deposition rate levels, it is higher for the reactive sputtering of the chromium target than for the tantalum target.

Finally, it is noted that the deposition rate did not decrease as quickly for the reactive sputtering of the zinc oxide target as for the metal targets when oxygen is added to the sputtering gas. This

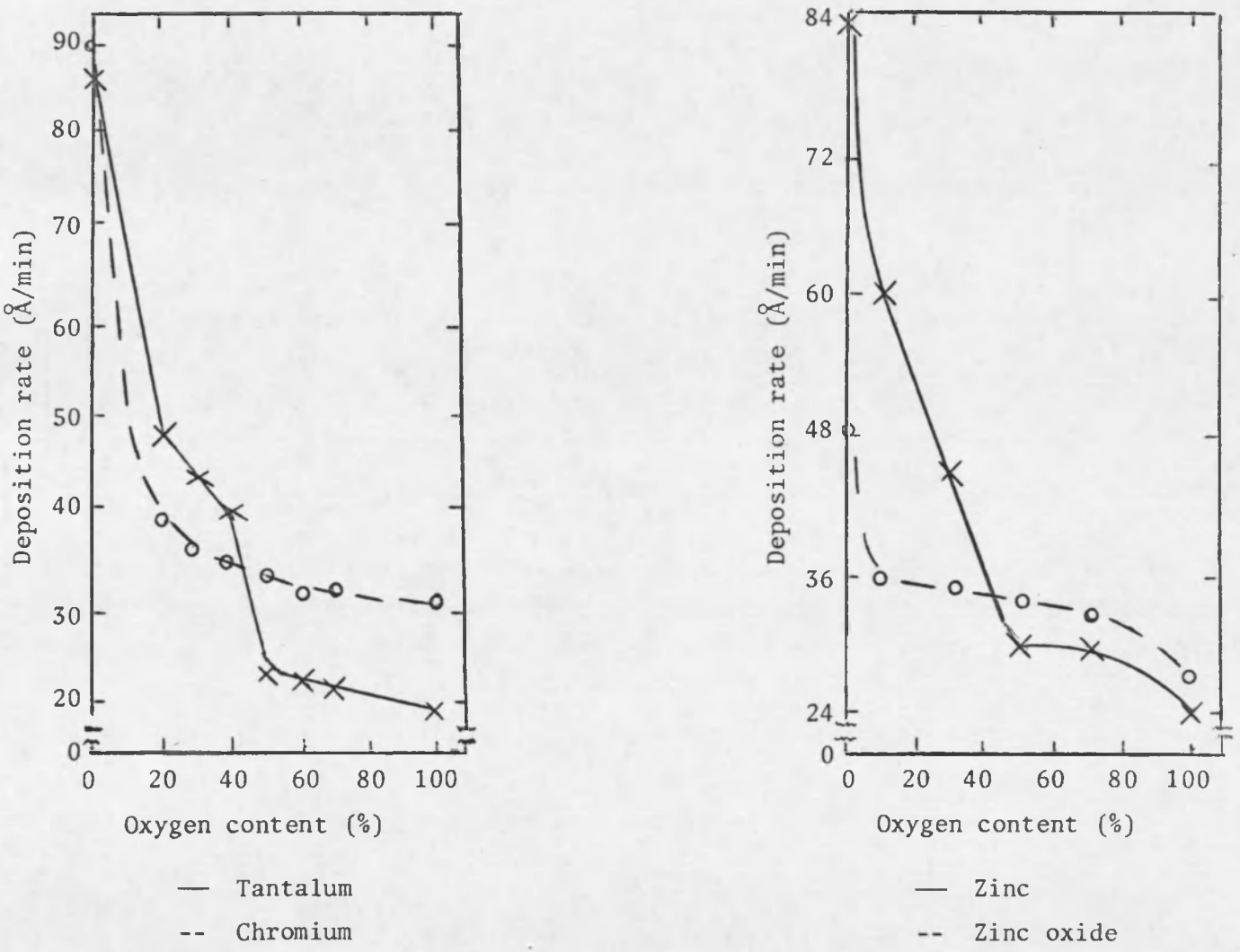


Fig. 11. Deposition Rate vs Oxygen Content for Tantalum, Chromium, Zinc, and Zinc Oxide.

occurs because it contains oxygen atoms, and because of the insulating nature of the target.

## Deposition Rate vs Pressure

The next parameter to be examined is the variation of the deposition rate with the pressure of the mixture. A 30/70 argon/oxygen mixture was used, i.e., 30% argon and 70% oxygen mixture of the sputtering gas. This mixture was selected because, as seen from Fig. 11, it is in this area that the deposition rate remained constant with increasing oxygen content. This is needed so that, if the oxygen content of the sputtering gas changes slightly, it will not affect the experimental result. Also, it was with this mixture that, by inspection, clear thin films could be deposited consistently.

From Figs. 12 and 13, it is seen that the variation in the deposition rate with pressure is similar to that observed when the targets are nonreactively sputtered. Also, as occurred previously, the deposition rate is dependent on the target-substrate separation. The amount of decrease in the deposition rate when the target-substrate separation increases is dependent on the deposited film. A large change in the deposition rate with increasing target-substrate separation is noticed for the deposited tantalum oxide films. A slightly smaller change is observed for the chromium oxide films and an even smaller change for the zinc oxide films. This result is expected when the atomic mass of the deposited films is considered. Tantalum pentoxide, $Ta_2O_5$, which is assumed to be the deposited film, has an atomic mass of 442. Chromium sesquioxide, $Cr_2O_3$, has an atomic mass of 152, and zinc oxide, ZnO, has

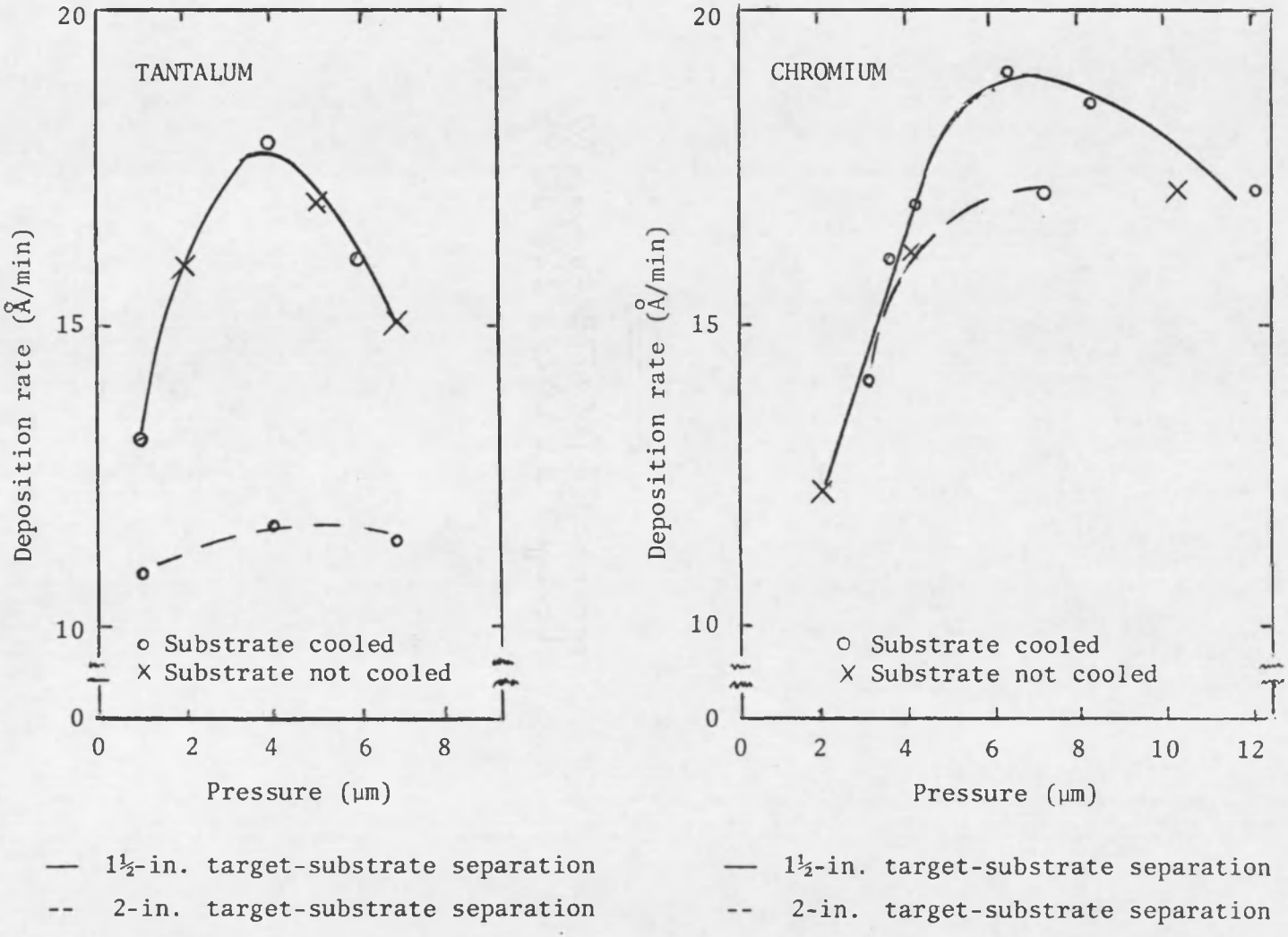


Fig. 12. Deposition Rate vs Pressure for the Reactive Sputtering of Tantalum and Chromium.

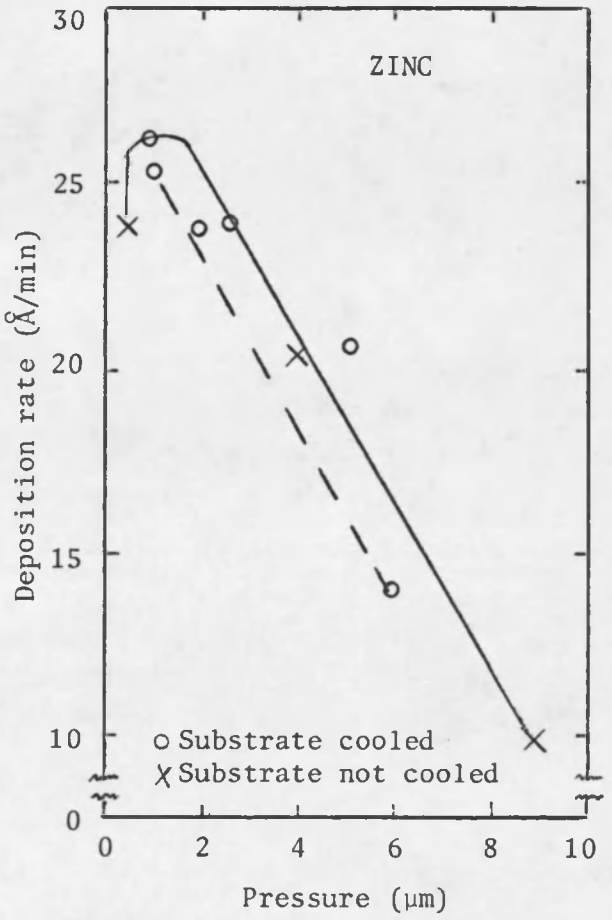


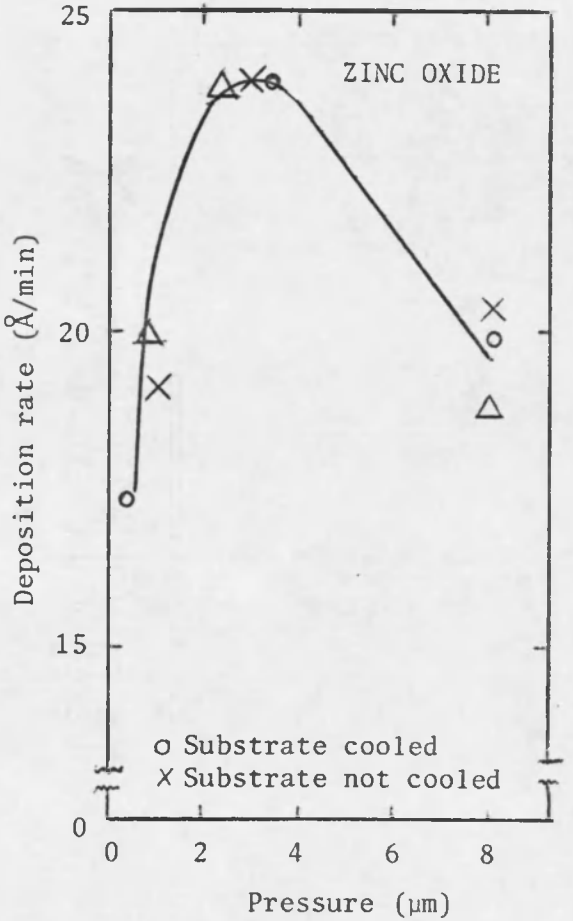


— 1½-in. target-substrate separation
-- 2-in. target-substrate separation

o X 1½-in. target-substrate separation
△ 2-in. target-substrate separation

Fig. 13. Deposition Rate vs Pressure for the Reactive Sputtering of Zinc and Zinc Oxide.

an atomic mass of 82 (*Handbook of Chemistry and Physics*, 1969, pp. B-83 to B-176). Because of the larger atomic mass, tantalum oxide would have a smaller mean free path, and therefore a larger decrease in the deposition rate would be observed when the target-substrate separation is increased. This result is consistent with the observation, as seen in Figs. 12 and 13, that the deposition rate increases as the atomic mass of the deposited film decreases.

From these curves it may be seen that the deposition rate is independent of whether or not the substrate is cooled. This is consistent with the nonreactive sputtering of the zinc oxide target discussed in the previous chapter.

## Deposition Rate vs Input Power

From Fig. 14, it is seen how the deposition rate varies as the input power to the target is increased. As with the nonreactive sputtering of the targets, the graphs are a plot of the deposition rate as a function of the power being supplied to each square centimeter of the target surface. An input power of 250 W corresponds to 10.4 $W/cm^2$ for the chromium target and 12.7 $W/cm^2$ for the tantalum, zinc, and zinc oxide targets. It is seen that chromium oxide has a faster deposition rate for a given input power than tantalum oxide, which is consistent with the results reported in Chapter 4 for the nonreactive sputtering of these targets. The deposition rates for the reactive sputtering of the zinc and zinc oxide targets are about the same. However, for the zinc oxide target, the increase in the deposition rate with increasing input power is not linear. This is due to the insulating nature of the target.

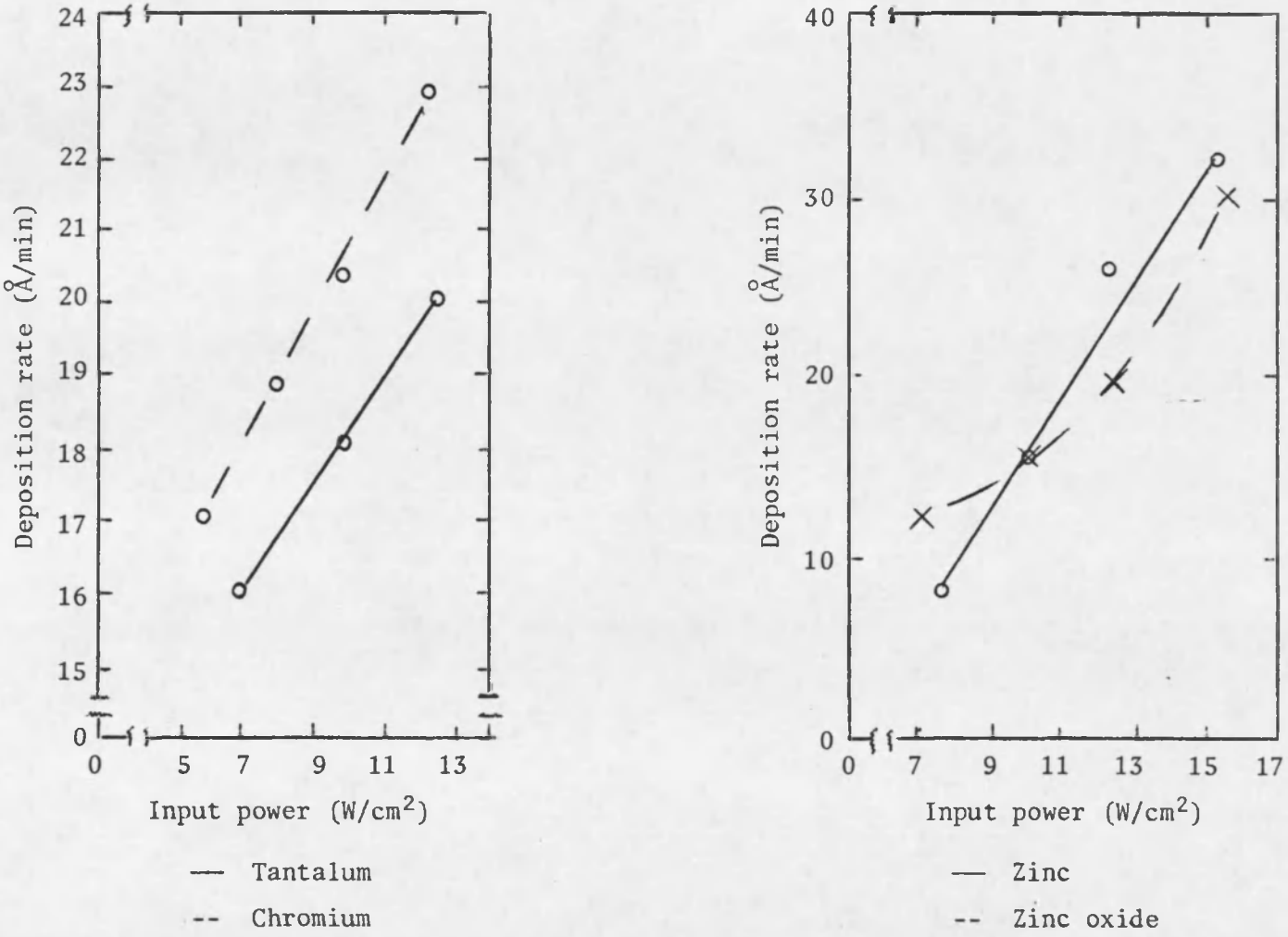


Fig. 14. Deposition Rate vs Input Power for the Reactive Sputtering of Tantalum, Chromium, Zinc, and Zinc Oxide.

## Thickness vs Time

The next parameter to be examined is the variation in the deposition rate with duration of deposition. As shown in Fig. 15, the deposition rate, which is the slope of the plotted curves, remained constant with increasing time. This is consistent with the results observed when these targets are nonreactively sputtered.

## Characteristic Deposition Rates

From Figs. 16 through 20, it is seen how the deposition rate varied on the substrate platform for each of the deposited films. This is shown for target-substrate separations of both 1½ in. and 2 in. The scale used for these diagrams is half the dimensions of the pattern as it appeared on the substrate platform. The deposition rates given are based on the interference color of the coated slides. These characteristic diagrams are the same with and without the substrate cooling. The diagrams indicate the trend in the variation of the deposition rate on the substrate, and they will change with pressure and gas flow in the sputtering chamber, and with the deposition time. The diagrams indicate the variation of the deposition rate on the substrate platform for the maximum deposition rate.

A general observation from these diagrams is that there exists, at a 1½-in. target-substrate separation, two spots on the substrate platform where the deposition rates are high. Except for the sputtering of chromium oxide and the nonreactive sputtering of the zinc oxide target, these spots disappear when the target-substrate separation increases to 2 in. These two spots occur near the arms of the conical cross and are

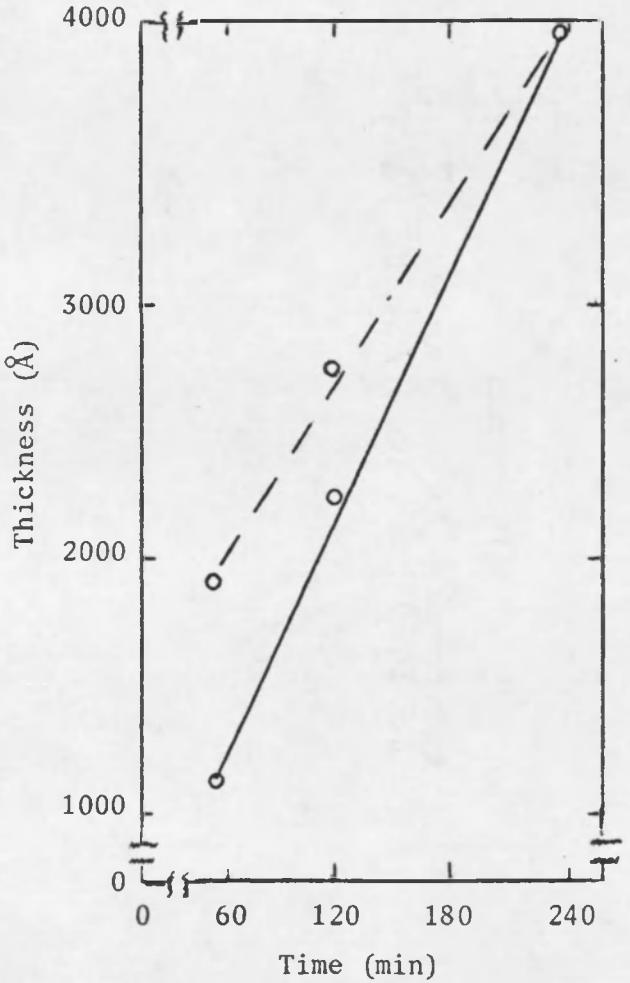


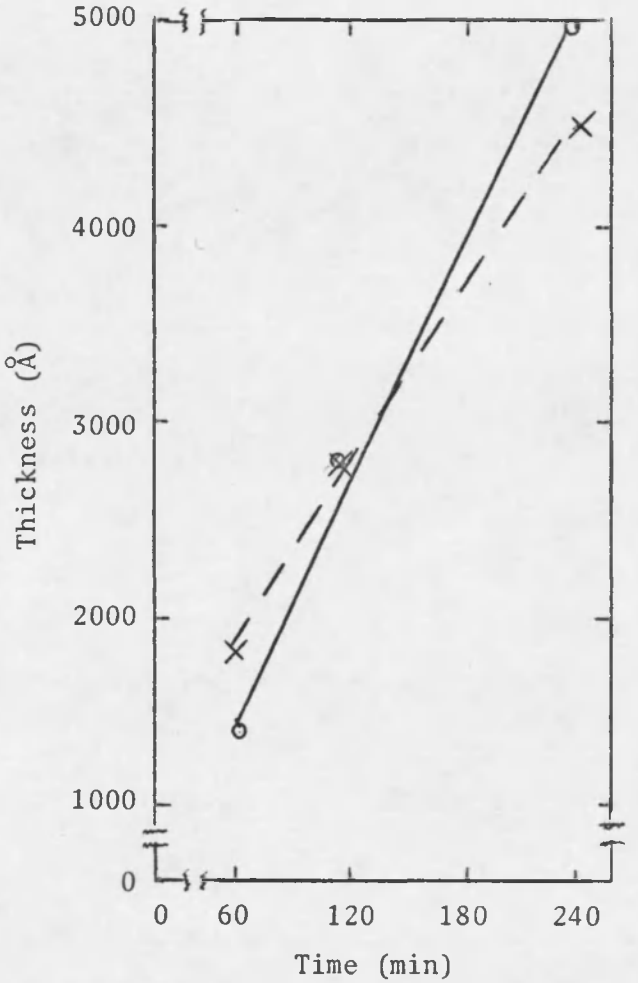


Fig. 15. Thickness vs Time for the Reactive Sputtering of Tantalum, Chromium, Zinc, and Zinc Oxide.

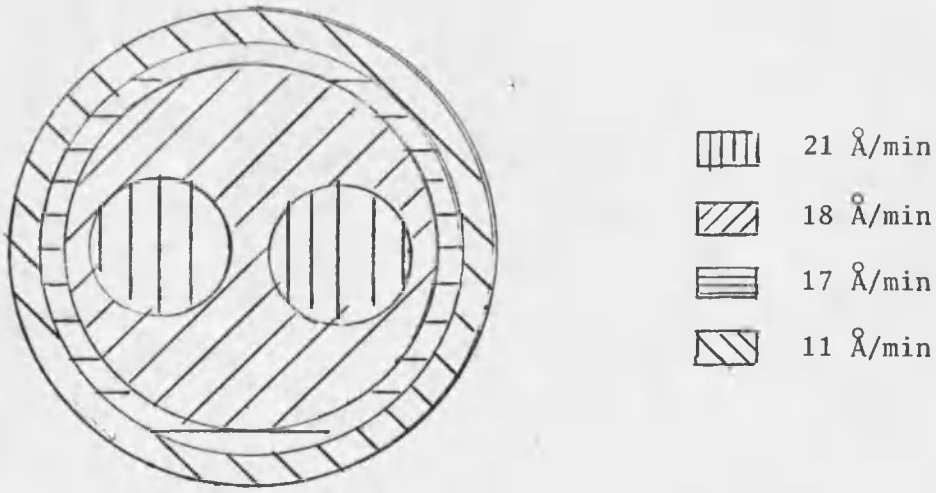


A. 1½-in. target-substrate separation.

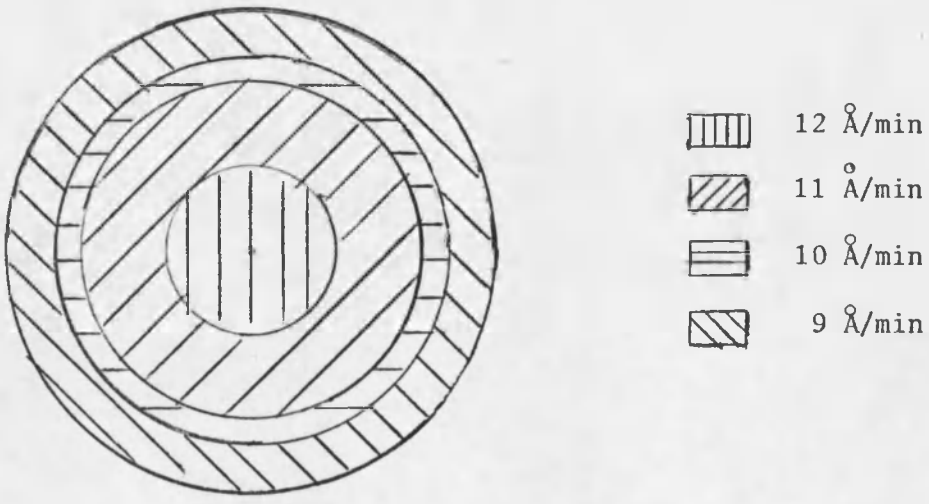


B. 2-in. target-substrate separation.

Fig. 16. Characteristic Deposition Rates for Tantalum Reactively Sputtered.

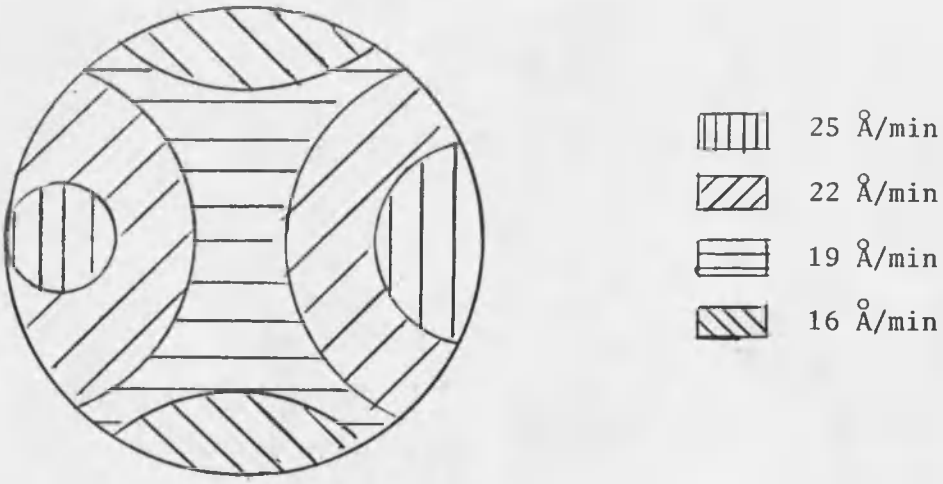


A. 1½-in. target-substrate separation.

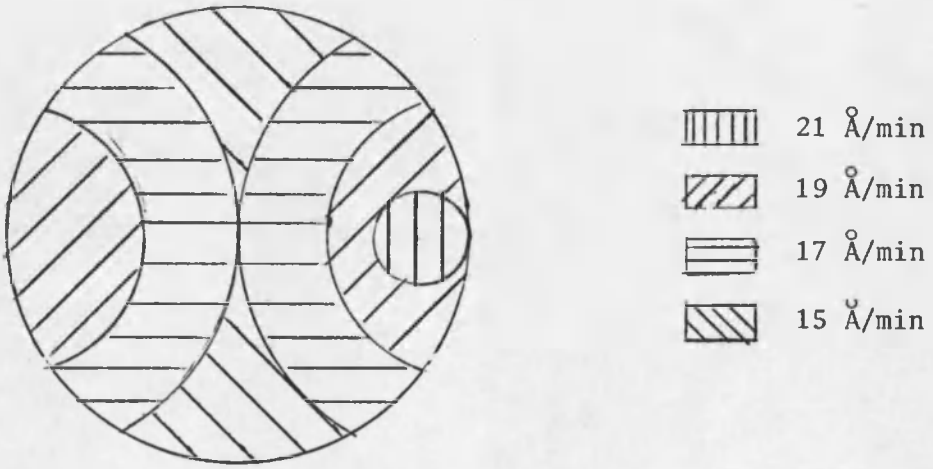


B. 2-in. target-substrate separation.

Fig. 17. Characteristic Deposition Rates for Chromium Reactively Sputtered.

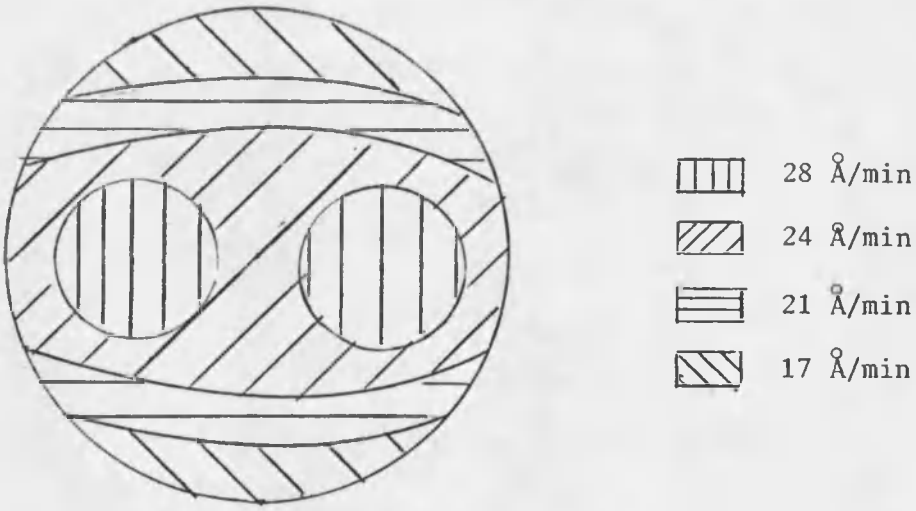


A. 1½-in. target-substrate separation.

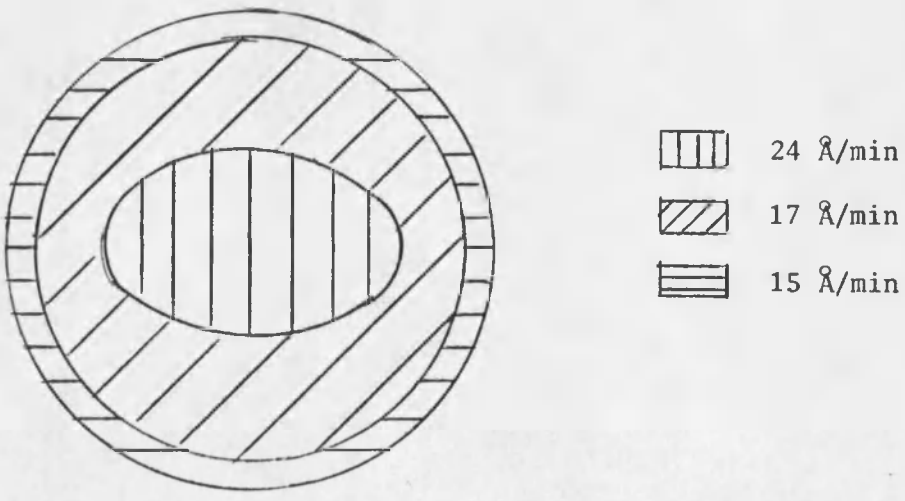


B. 2-in. target-substrate separation.

Fig. 18. Characteristic Deposition Rates for Zinc Reactively Sputtered.

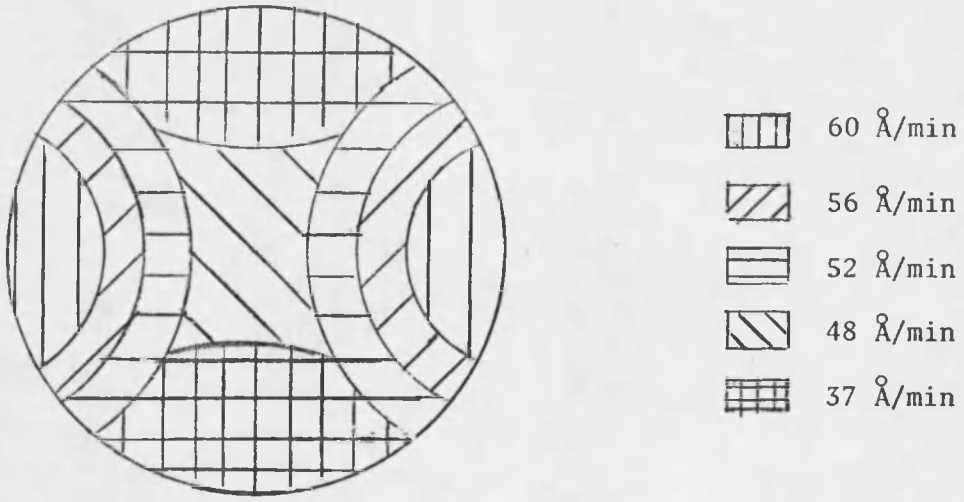


A. 1½-in. target-substrate separation.

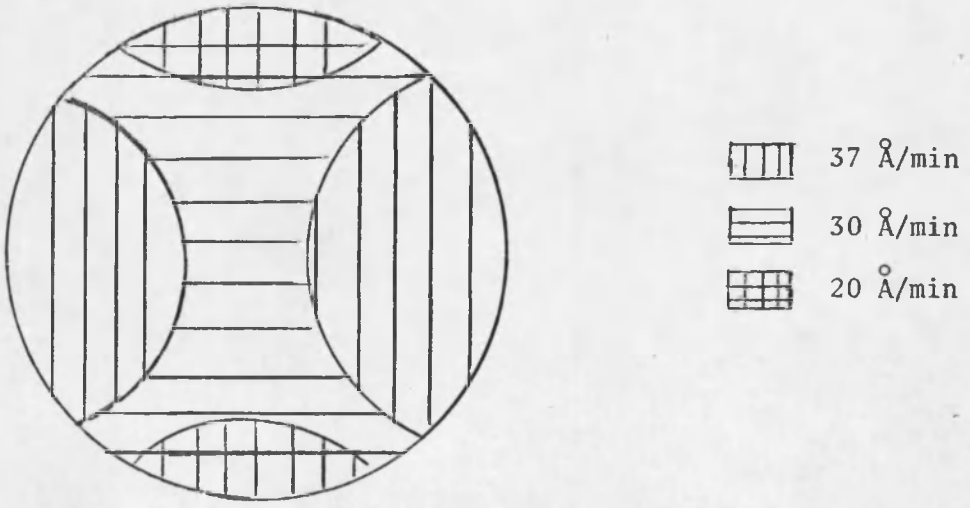


B. 2-in. target-substrate separation.

Fig. 19. Characteristic Deposition Rates for Zinc Oxide.

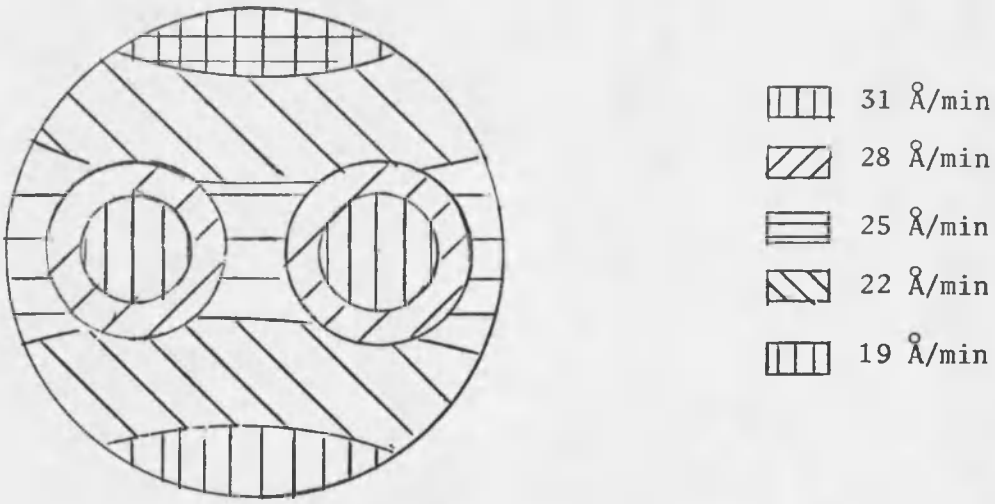


A. 1½-in. target-substrate separation.

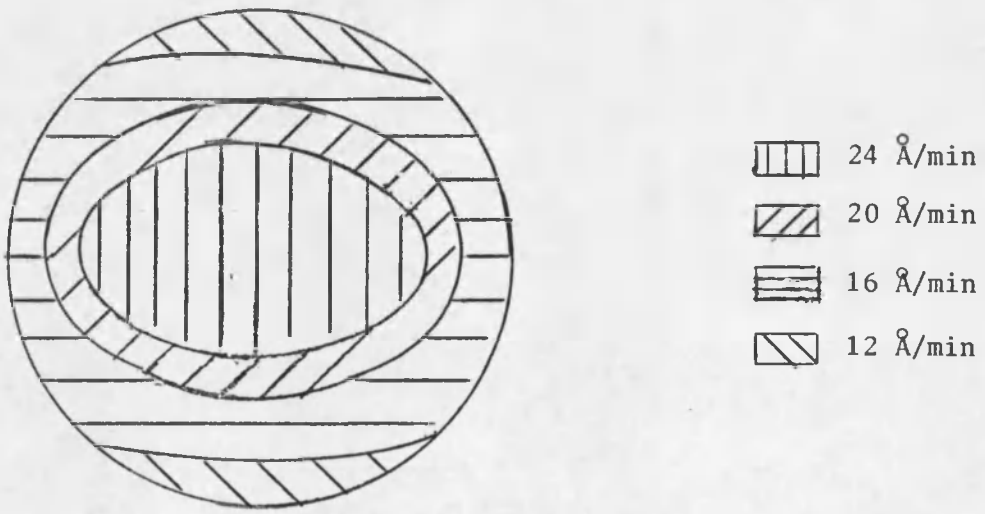


B. 2-in. target-substrate separation.

Fig. 20. Characteristic Deposition Rates for Zinc Oxide Reactively Sputtered.

apparently due to the concentration of the rf field near the arms of the conical cross. This results in a higher ion concentration in this region, which leads to higher deposition rates. When the target-substrate separation is increased to 2 in., there is room for a more even distribution of the sputtered atoms, and these two spots disappear. However, these spots will not disappear for the reactive sputtering of the chromium target because it is 5½ in. in diameter, compared to the 5-in. diameter of the other targets. Because the chromium target is closer to the arms of the conical cross, the rf field concentration is greater, and this will tend to keep the sputtered atoms from being evenly distributed when the target-substrate separation is increased.

## Temperature of the Substrate

As discussed previously, the deposition rate did not depend on whether or not the substrate is cooled. It was observed that the temperature of the substrate remained constant after about the first five min of the experimental trial. The variation in the temperature of the substrate after this time was only about ±3°C. From Table 2, it is seen that the temperature of the substrate changed with the different sputtered films and with the target-substrate separation. These changes are apparently due to the amount of energy transferred to the substrate by the sputtered atoms. When the target-substrate separation is increased by ½ in., the substrate would be cooler because of the extra collisions and further loss of energy of the sputtered atoms in traveling the extra ½ in.

Table 2. Table of Temperature of Substrate.

| | Target-substrate separation | | | |
|---|---|---|---|---|
| | Substrate cooled | | Substrate uncooled | |
| Deposited film | 1½ in. | 2 in. | 1½ in. | 2 in. |
| Tantalum reactively sputtered | 73°C | 70°C | 115°C | 106°C |
| Chromium reactively sputtered | 56°C | 54°C | 108°C | 100°C |
| Zinc reactively sputtered | 60°C | 60°C | 93°C | 85°C |
| Zinc oxide | 71°C | 53°C | 98°C | 97°C |
| Zinc oxide reactively sputtered | 68°C | 55°C | 92°C | 92°C |

## Index of Refraction

The index of refraction of the deposited films was measured using spectrophotometer transmission curves. Appendix C describes how the calculation for the index of refraction was performed.

As seen in Table 3, the refractive index varied with increasing oxygen content in the sputtering gas. Depending on the target element, the results indicate that the index of refraction remained constant after the oxygen content of the sputtering gas reached 50% to 60%. This result is expected because the properties of the deposited films should change with increasing oxygen content in the sputtering gas. This should occur up to the point where enough reactive gas is present in the sputtering chamber to form the compound film. The deposited films became noticeably less absorbing when the oxygen content reached 50% to 60%. The work for this thesis was done for optical integrated circuits, and

absorbing films are not of interest. Thus, no attempt was made to obtain further information from these films.

Table 3. Index of Refraction as a Function of Oxygen Content in Sputtering Gas.

| Oxygen content, percent | Thickness, angstroms | Index of refraction | Wavelength, angstroms |
|---|---|---|---|
| | Tantalum Reactively Sputtered | | |
| 10 | 3945 | 1.78 | 7000 |
| 20 | 3000 | 2.04 | 4900 |
| 30 | 2690 | 2.05 | 5500 |
| 40 | 2370 | 2.11 | 5000 |
| 70 | 1250 | 2.14 | 5350 |
| | Chromium Reactively Sputtered | | |
| 10 | 3260 | 3.72 | 5400 |
| 20 | 2220 | 3.80 | 6800 |
| 50 | 1900 | 2.77 | 7000 |
| 60 | 1870 | 2.70 | 6750 |
| 70 | 2410 | 2.70 | 6500 |
| | Zinc Reactively Sputtered | | |
| 30 | 2740 | 1.75 | 4850 |
| 50 | 1750 | 1.80 | 6250 |
| 70 | 2660 | 2.11 | 5600 |
| 100 | 1250 | 2.10 | 5240 |
| | Zinc Oxide Reactively Sputtered | | |
| 30 | 2110 | 1.87 | 5250 |
| 50 | 2000 | 1.97 | 5250 |
| 70 | 4640 | 2.02 | 5350 |

Using a standard oxygen content of 70%, the index of refraction of the deposited films for various thicknesses is seen in Table 4. Because the measured refractive index was observed to be independent of wavelength and thickness, the values in this table are averaged. Comparing this average to the values of the refractive index from the *Handbook of Chemistry and Physics* (1969, pp. B-83 to B-176) at 6328 Å, the following results are obtained: When the substrate is cooled, the average refractive index for tantalum oxide is 2.14, and the index of refraction for tantalum pentoxide is 2.25. For the deposited chromium oxide films, the average refractive index is 2.70, and for chromium sesquioxide the average is 2.55. Zinc oxide has a refractive index of 1.99. When the zinc oxide target is nonreactively sputtered, the average refractive index is measured to be 2.03, and when it is reactively sputtered it is measured to be 2.02. When the zinc target is reactively sputtered, the average refractive index is 2.01.

When the substrate is not cooled, the refractive index changes. as shown in Table 5. For tantalum oxide, chromium oxide, and the nonreactive sputtering of the zinc oxide target, the refractive index is lower than when the substrate is cooled. But it is higher when the zinc target and the zinc oxide target are reactively sputtered.

## Sheet Resistance

A measurement of the sheet resistance for the films deposited by the reactive sputtering of the targets was attempted. However, only when the tantalum and chromium targets are reactively sputtered in a 90/10 argon/oxygen mixture is any measurement possible. For the

Table 4. Index of Refraction as a Function of Thickness When the Substrate Is Cooled.

| Thickness angstroms | Index of refraction | Wavelength, angstroms |
|---|---|---|
| | Tantalum Reactively Sputtered | |
| 1250 | 2.14 | 5350 |
| 1650 | 2.19 | 4800 |
| 2050 | 2.10 | 4300 |
| 2180 | 2.14 | 4650 |
| | Ave.: 2.14 | |
| | Chromium Reactively Sputtered | |
| 1870 | 2.67 | 6600 |
| 2410 | 2.70 | 6500 |
| 2500 | 2.76 | 6900 |
| | Ave.: 2.70 | |
| | Zinc Reactively Sputtered | |
| 2660 | 2.11 | 5600 |
| 3370 | 1.93 | 6500 |
| 5000 | 2.00 | 5000 |
| | Ave.: 2.01 | |
| | Zinc Oxide | |
| 1730 | 2.01 | 7000 |
| 2430 | 2.14 | 5200 |
| 4570 | 1.93 | 5900 |
| | Ave.: 2.03 | |
| | Zinc Oxide Reactively Sputtered | |
| 2090 | 2.08 | 4350 |
| 3380 | 1.98 | 5350 |
| 4640 | 2.02 | 5350 |
| | Ave.: 2.02 | |

Table 5. Index of Refraction as a Function of Thickness When Substrate Is Not Cooled.

| Thickness, angstroms | Index of refraction | Wavelength, angstroms |
|---|---|---|
| | Tantalum Reactively Sputtered | |
| 1250 | 1.90 | 4750 |
| | Chromium Reactively Sputtered | |
| 1780 | 1.95 | 6900 |
| 1850 | 1.95 | 7200 |
| | Ave.: 1.95 | |
| | Zinc Reactively Sputtered | |
| 1200 | 2.23 | 5350 |
| 2530 | 2.22 | 5600 |
| 2850 | 1.99 | 5650 |
| | Ave.: 2.14 | |
| | Zinc Oxide | |
| 1950 | 1.79 | 7000 |
| 1980 | 1.77 | 7000 |
| | Ave.: 1.78 | |
| | Zinc Oxide Reactively Sputtered | |
| 2010 | 2.10 | 4750 |
| 2090 | 2.10 | 5900 |
| 2770 | 2.20 | 6100 |
| | Ave.: 2.13 | |

tantalum oxide film in a 90/10 mixture, the sheet resistance is 32 Ω per square, and for a tantalum film of the same thickness the sheet resistance is 8 Ω per square. This is a 400% increase in the sheet resistance

with a 10% increase in the oxygen content in the sputtering gas. For the chromium oxide film deposited in a 90/10 mixture, the sheet resistance is 21 Ω per square, and for a chromium film with the same thickness the sheet resistance is 7 Ω per square. This is a 300% increase in the sheet resistance with a 10% increase in the oxygen content in the sputtering gas. As explained previously, these results are expected because as oxygen is added to the sputtering gas, the films should become more resistive owing to the nature of dielectric films. The results show the sensitivity of the sheet resistance to the amounts of reactive gases present in the system.

## Summary of the Reactive Sputtering of Tantalum, Chromium, Zinc, and Zinc Oxide

Some of the characteristics of rf reactive sputtering have been studied. As expected, the deposition rate decreases with increasing oxygen content in the sputtering gas until a 50/50 argon/oxygen mixture is present in the gas. At this mixture, the deposition rate remains constant with increasing oxygen content of the sputtering gas. It is also observed that the refractive index remains constant after about a 50/50 argon/oxygen mixture in the sputtering gas. These two results indicate that the oxidation of the sputtered target atoms is complete after 50% of the sputtering gas contains oxygen. It is observed that the refractive index does change when the substrate is not cooled. Also, there is a large increase in the sheet resistance of the deposited film when oxygen is added to the sputtering gas.

The graphs of the deposition rate as a function of pressure for the reactive sputtering of the targets are similar to those for the

nonreactive sputtering. Also, the graphs of the deposition rate as a function of input power, and the thickness of the deposited films as a function of time, are similar to the observations for the nonreactive sputtering of the same targets.

Finally, it is noticed that the deposition rate varies on the substrate platform. There seems to be a concentration of the rf power near the arms of the conical cross. This is apparently a phenomenon of the system used for these investigations that could be corrected through the use of a different sputtering chamber configuration.

# CHAPTER 6

## CONCLUSIONS AND RECOMMENDATIONS

The purpose of this thesis, as stated in Chapter 1, is to investigate rf nonreactive and rf reactive sputtering with the system assembled in the Solid State Engineering Laboratory. By examining the four different targets in these two modes of sputtering, the characteristics of rf sputtering with this system were observed. It has been shown that these characteristics are consistent with the theory of rf sputtering and that this system can be used to sputter both metal and insulating targets. The results presented in this thesis have been checked and found to be reproducible and consistent.

The following results were obtained using this rf sputtering system. The deposition rate depends on the pressure of the gas in the sputtering chamber. The pressure for the maximum deposition rate and the value of the maximum deposition rate both depend on the target material, target-substrate separation, and oxygen content of the sputtering gas. They are not dependent on whether or not the substrate is cooled.

The deposition rate increases linearly as the input power to the targets is increased. This occurred for both the nonreactive and reactive sputtering of the tantalum, chromium, zinc, and zinc-oxide targets investigated. The rate of change of this increase depends on the target material.

The thickness of the films also increases linearly with deposition time. This is observed for both the nonreactive and reactive sputtering of these targets. The rate of change of the thickness with time depends on the target material.

The sheet resistance of the metal films decreases as the thickness of the films increases. However, the measured sheet resistance is higher than theoretically predicted. It was also observed that the sheet resistance increases greatly when small amounts of oxygen are added to the sputtering gas.

For the rf reactive sputtering of the four targets, the deposition rate decreases with increasing oxygen content in the sputtering gas. This occurs until enough oxygen is present in the sputtering atmosphere that the sputtered atoms are completely oxidized, at which time the deposition rate remains constant. The fact that the sputtered atoms are completely oxidized is verified when the index of refraction of the deposited films is measured. The deposition rate remains constant with increasing oxygen content in the sputtering gas at the same oxygen mixture where the refractive index remains constant.

It was found that, when the substrate is not cooled, the refractive index is different than when it is cooled. This indicates that a different material forms on the substrate.

Finally, the deposition rate varies on the substrate platform. This variation depends not only on the target-substrate separation but also on the size of the target and the target material.

The dielectric films were examined for their use in guiding visible light waves. The tantalum oxide and the zinc oxide films were

found to have high attenuation of the light wave, around 50 dB/cm. Zinc oxide films are reported to have an attenuation at about this value. Tantalum oxide films are reported to have lower attenuation of the energy of the light. However, these films were not produced by the reactive sputtering of a tantalum target, which could be the reason the films deposited for this thesis exhibited higher attenuations (Tien, 1971, pp. 2403-2406). Not reported in this thesis, but examined for their waveguiding properties, were glass films that were nonreactively sputtered. These films did exhibit, as expected, low attenuation of the light wave, especially when deposited on quartz substrates. Thus, films deposited by rf sputtering could be used in optical integrated circuits.

The results reported in this thesis indicate that sputtering is a valuable method of depositing thin films. However, a better system than the one used for the work on this project is needed because there is too much power lost in the components of this system. The rf network, from the transmitter to the input wiring, needs to be redesigned so that the maximum power goes into sputtering the targets, and the conical cross needs to be replaced with a symmetrical sputtering chamber. With a properly designed sputtering system, the deposition rates of the sputtered films should be comparable to the deposition rates attained by evaporation. But this cannot be achieved with the system presently available. A better system is needed in order to accomplish all of the benefits of sputtering thin films. However, the results presented in this thesis demonstrate the value and use of rf sputtering.

# APPENDIX A

## OPERATING PROCEDURES FOR RF SPUTTERING

The following procedures were used to rf sputter the films in this thesis:

1. Place glass and/or silicon substrate on the substrate platform.

2. Place plate on top of Pyrex conical cross.

3. Open valve to the roughing pump after making sure foreline valve to the diffusion pump is closed and bleed valve on roughing pump is open.

4. When the pressure inside conical cross reaches 300 μm, which should take less than a minute, close bleed valve on the roughing pump.

5. Allow the vacuum system to rough down until foreline reads less than 10 μm.

6. Open foreline valve to the diffusion pump.

7. When the conical cross reaches a pressure of less than 10 μm, close valve to the roughing pump and open valve to the diffusion pump.

8. Pump system down to about $5 \times 10^{-6}$ Torr ($10^{-3}$ μm).

9. Close valve to the diffusion pump and open valve to the roughing pump.

10. Raise pressure in the conical cross to at least 10 μm by opening micrometer valve to the gas tanks, mixing the gases as desired.

11. After turning the rf unit on, set the transmitter to the desired input power. The transmitter is 60% efficient. Bring the pressure of the sputtering gas mixture to the desired level by opening or closing the micrometer valve. The rf power affects the Hughes meter. The effect is dependent on the amount of rf power and the matching of the load. Match the output load with the input load by turning the variable capacitor until the standing wave ratio (SWR) is less than the value of two. Varying the copper coils will vary the inductance. *Note*: Make sure the power is off before moving these coils.

12. Sputter for the desired time.

13. When through sputtering, turn the rf unit off, pull the pressure out of the gas feed lines by turning off the gas supplies, close the foreline valve to the diffusion pump, and open the micrometer valve.

14. Close the valve to the roughing pump and bring the conical cross to atmospheric pressure.

15. Take the plate off the top of the Pyrex conical cross and remove the substrates.

## APPENDIX B

## PROCEDURES FOR MEASURING THE FILM THICKNESS

The thickness of the deposited films was measured by using Fizeau fringes, which are fringes of constant thickness.

1. To measure the thickness of the film, a step must be made in the film. This was done by placing a glass cover slide over part of the substrate before depositing the film. Thus, after deposition, a step equal to the thickness of the film is created.

2. The film was then overcoated with another film that had high reflectance.

3. The overcoated film was then viewed under a Fizeau interferometric microscope.

4. The step creates a displacement in the fringes. Using movable cross hairs in the eyepiece of this microscope and a micrometer screw, this displacement was measured. The thickness of the film was determined using the relationship

$$t = (d/w)(\lambda/2)$$

where

$t$ is the thickness of the film

$d$ is the displacement of the fringes, which is measured using the micrometer screw

$w$ is the separation between successive minima, which is measured using the micrometer screw

$\lambda$ is the wavelength of the monochromatic light used to produce the fringes.

For more details on the theory of measuring the thickness of thin films using Fizeau fringes, see Heavens (1965, pp. 106-111).

## APPENDIX C

## PROCEDURES FOR MEASURING THE REFRACTIVE INDEX

The index of refraction was measured using spectrophotometer transmission curves.

1. The deposited film was placed in one beam of the light in a spectrophotometer. A bare substrate was placed in the other beam of light in the spectrophotometer.

2. The intensity of the transmitted light through the film and substrate was measured relative to the intensity of the light through the substrate alone. Thus the effect of the substrate on the intensity of the transmitted light is negated. This relative intensity is measured as a function of the wavelength of the light in the spectrophotometer.

3. At the wavelength where the maximum intensity occurred, the refractive index was calculated from the relationship

$$n = m\lambda/2t$$

where

$n$ is the index of refraction

$\lambda$ is the wavelength at maximum intensity

$t$ is the thickness of the film (see Appendix B)

$m$ is the order number ($m$ = 0,1,2,...); the order number was determined by noting the color changes on a silicon wafer during deposition; for most of the deposited films, the wavelength used corresponds to first order.

For more details on the theory of measuring the index of refraction with a spectrophotometer, see Heavens (1965, p. 115).

## REFERENCES


Blevis, Earl H., 1964 (Feb.), "Glow Discharge Sputtering--Theory and Practice," distributed by R. D. Mathis Co.

Blevis, Earl H., 1965 (Feb.), "Hot Cathode and Radio Frequency Sputtering," distributed by R. D. Mathis Co.

Cash, John H., James A. Cunningham, and Joe P. Keene, 1967, "RF Sputtering of Metals," presented at Second Symposium on the Deposition of Thin Films by Sputtering, June 6 and 7, 1967.

Davidse, P. D., 1966, "Theory and Practice of RF Sputtering," presented at Symposium on the Deposition of Thin Films by Sputtering, June 9, 1966.

Froemel, John G., and Meyer Sapoff, 1967, "Pulse Plasma Sputtering," presented at Second Symposium on the Deposition of Thin Films by Sputtering, June 6 and 7, 1967.

*Handbook of Chemistry and Physics*, 1969, Cleveland, Chemical Rubber Publishing Company.

Heavens, O. S., 1965, *Optical Properties of Thin Solid Films*, New York, Dover Publications, Inc.

Maissel, Leon I., and Reinhard Glang, 1970, *Handbook of Thin Film Technology*, New York, McGraw-Hill Book Company.

Murray, G. T., and Walter Class, 1970, "Materials and Construction of Sputtering Target Assemblies," presented at Conference and School on Sputtering for Electronics, January 25-28, 1970.

Nickerson, John W., and Roger Moseson, 1965 (Mar.), "Low Energy Sputtering," reprinted from Research/Development, by Consolidated Vacuum Corporation.

Schwartz, Newton, 1966, "Sputtered Resistive and Dielectric Films," presented at Symposium on the Deposition of Thin Films by Sputtering, June 9, 1966.

Seeman, James M., 1965, "Ion-Sputtered Thin Films," presented at Sixth Annual Structures and Materials Conference of the American Institute of Aeronautics and Astronautics, April 5-7, 1965.

Tien, P. K., 1971, "Light Waves in Thin Films and Integrated Optics," Appl. Opt. 10(11):2395-2413.

Vossen, J. L., and J. J. O'Neill, Jr., 1968 (June), "RF Sputtering Processes," RCA Review, pp. 149-179.

Vranty, F., and D. J. Harington, 1965, "Tantalum Films Deposited by Asymmetric AC Sputtering," J. Electrochemical Soc. 112(5): 484-489.